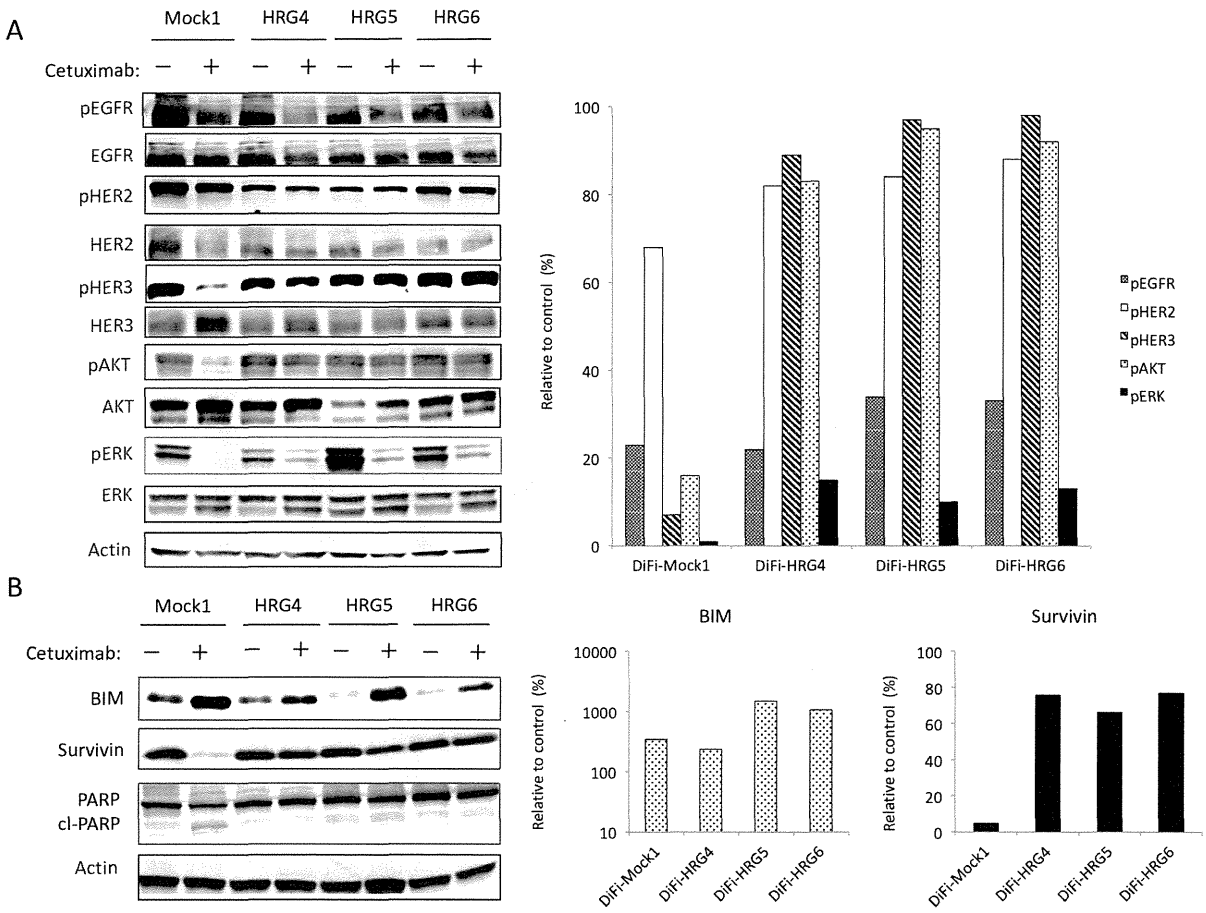

Figure 2: Effects of cetuximab on intracellular signaling and the expression of apoptosis-related proteins in DiFi isogenic cell lines. DiFi-Mock1, DiFi-HRG4, DiFi-HRG5, or DiFi-HRG6 cells were cultured overnight in medium containing 10% serum and then incubated for 6 h **(A)** or 24 h **(B)** in serum-free medium with or without cetuximab (10 μg/mL), after which cell lysates were prepared and subjected to immunoblot analysis with antibodies to phosphorylated (p) or total forms of the indicated proteins (left panels). A band corresponding to the cleaved (cl) form of PARP is indicated. The intensity of the bands corresponding to phosphorylated forms of EGFR, HER2, HER3, AKT, and ERK (A) or to BIM and survivin (B) was normalized by that of the corresponding total proteins or β-actin, respectively, and then expressed relative to the corresponding value for control cells not exposed to cetuximab (right panels).

treatment with patritumab and cetuximab *in vivo*, we injected nude mice with DiFi-Mock1 or DiFi-HRG4 cells to allow the formation of tumor xenografts. Whereas cetuximab alone markedly inhibited the growth of DiFi-Mock1 xenografts (Fig. 4A), DiFi-HRG4 xenografts were resistant to this drug (Fig. 4B). Patritumab alone had little effect on the growth of tumors formed by either cell line. However, the combination of cetuximab and patritumab induced substantial regression of DiFi-HRG4 xenografts (Fig. 4B). These results thus suggested that heregulin produced by colorectal cancer tumors harboring wild-type *KRAS* induces cetuximab resistance, and that combination therapy with cetuximab and patritumab overcomes such resistance *in vivo*.

DISCUSSION

Resistance to cetuximab is a major problem in the treatment of colorectal cancer. Although various mechanisms of cetuximab resistance have been identified [1–7, 17–20], the optimal treatment strategies for mCRC patients who show resistance to this drug remain unclear. We previously showed that tumor-derived heregulin mediates cetuximab resistance in preclinical models [8]. High levels of heregulin were also associated with a poor clinical outcome in mCRC patients treated with cetuximab-based regimens [8]. Moreover, increased heregulin levels were observed in such patients after the development of clinical resistance to cetuximab-based

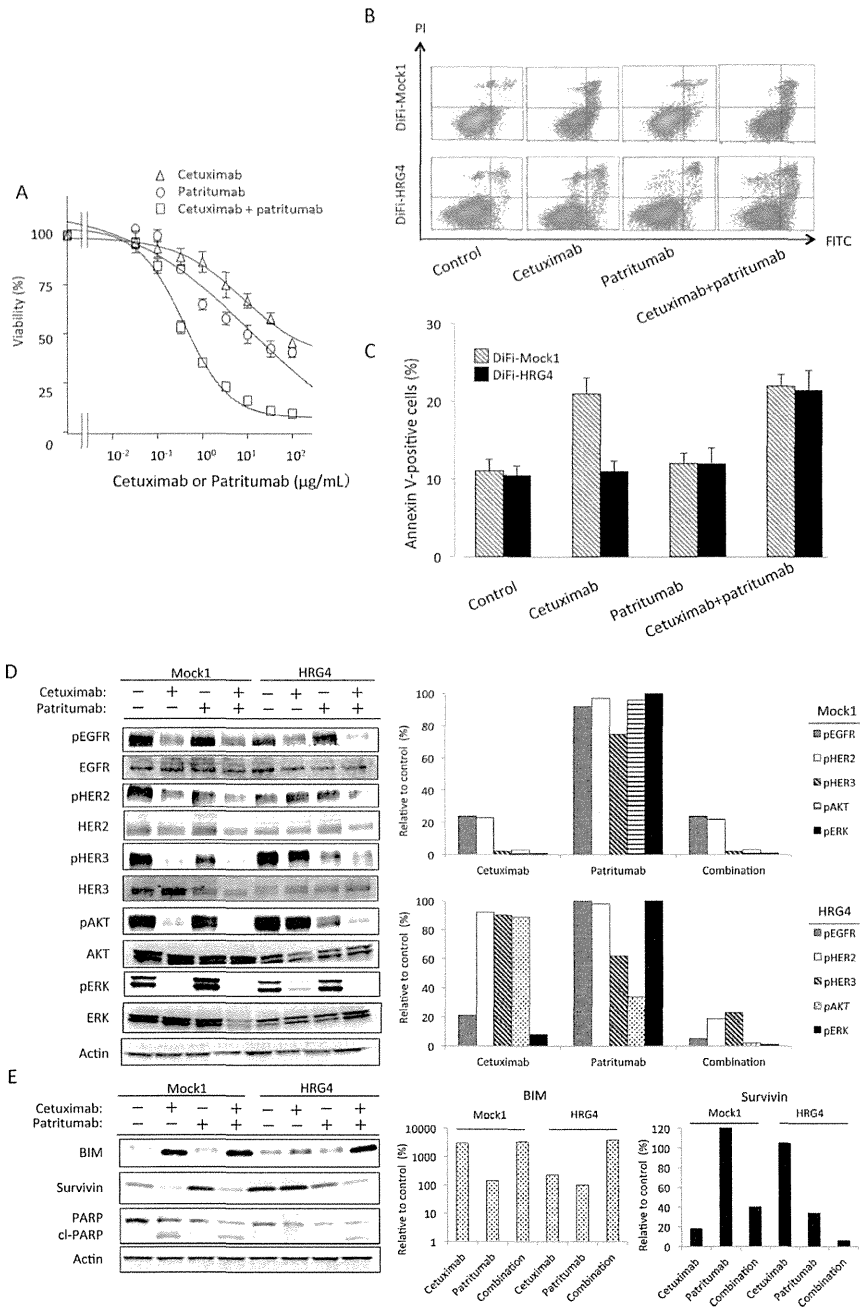

Figure 3: Effect of patritumab on heregulin-mediated cetuximab resistance in DiFi-HRG cells *in vitro*. **(A)** DiFi-HRG4 cells were incubated for 5 days with cetuximab alone, patritumab alone, or the combination of both drugs at the indicated concentrations, after which cell viability was assessed. Data are means ± SE from three independent experiments. **(B, C)** DiFi-Mock1 or DiFi-HRG4 cells were cultured overnight in medium containing 10% serum and then incubated for 48 h in the absence or presence of cetuximab alone (10 μg/mL), patritumab alone (10 μg/mL), or the combination of both drugs in serum-free medium, after which the number of apoptotic cells was determined by staining with propidium iodide (PI) and fluorescein isothiocyanate (FITC)–labeled annexin V followed by flow cytometry. Representative flow cytometric profiles are shown in (B), and quantitative data (means ± SE of three independent experiments) are shown in (C). **(D, E)** DiFi-Mock1 or DiFi-HRG4 cells were cultured overnight in medium containing 10% serum and then incubated for 6 h (D) or 48 h (E) in the absence or presence of cetuximab alone (10 μg/mL), patritumab alone (10 μg/mL), or the combination of both drugs in serum-free medium, after which cell lysates were prepared and subjected to immunoblot analysis with antibodies to the indicated proteins (left panels). The intensity of the bands corresponding to phosphorylated forms of EGFR, HER2, HER3, AKT, and ERK (D) or to BIM and survivin (E) was normalized by that of the corresponding total proteins or β-actin, respectively, and then expressed relative to the corresponding value for control cells not exposed to drug (right panels).

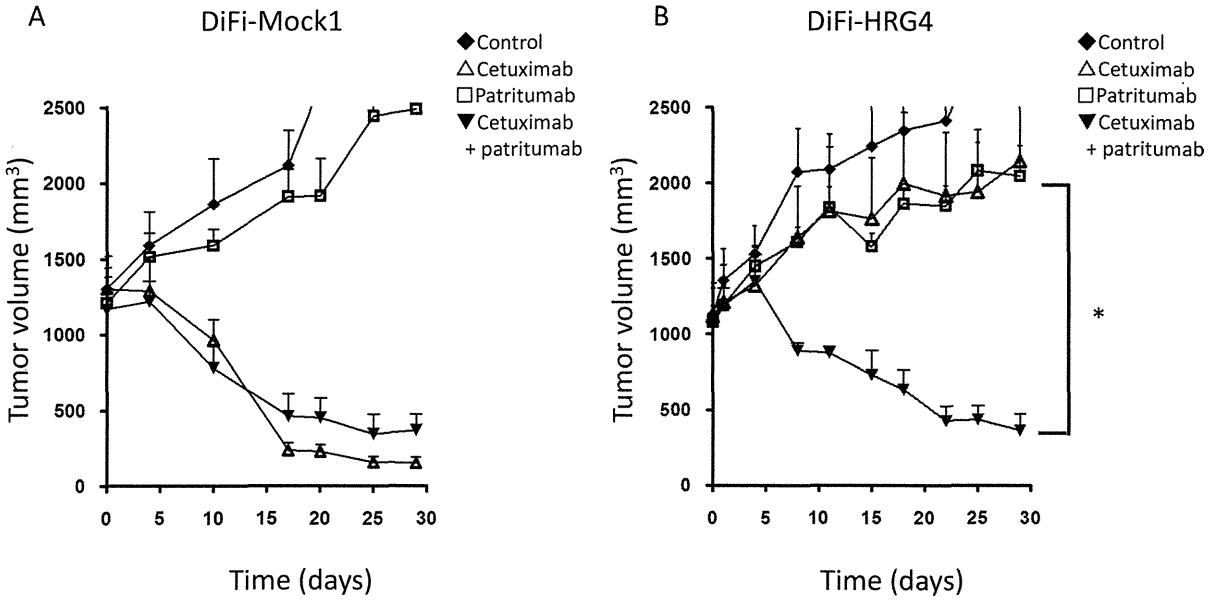

Figure 4: Effects of cetuximab, patritumab, and the combination of both drugs on the growth of DiFi-HRG tumor xenografts *in vivo*. Nude mice with tumor xenografts established by subcutaneous injection of DiFi-Mock1 **(A)** or DiFi-HRG4 **(B)** cells were treated for 4 weeks with vehicle (control), cetuximab (1.0 mg/body), patritumab (1.0 mg/body), or both drugs, as described in Materials and Methods. Tumor volume was determined at the indicated times after the onset of treatment. Data are means ± SE from six mice per group. $^*P < 0.05$ for comparison of the combination of both drugs with cetuximab alone or patritumab alone (Student's *t* test).

therapy [8]. Effective treatment options to overcome cetuximab resistance mediated by heregulin are thus urgently required.

We have here established heregulin-overexpressing sublines of DiFi cells (DiFi-HRG cells) and shown that these cells are resistant to cetuximab both *in vitro* and *in vivo*. Whereas the amount of the transmembrane form of heregulin was substantially higher in DiFi-HRG4 cells than in DiFi-HRG5 or DiFi-HRG6 cells (Fig. 1A), these three cell lines appeared to release similar amounts of the soluble form of heregulin into the culture medium (Fig. 1B). This difference in the relative abundance of the transmembrane and soluble forms of heregulin among DiFi-HRG cell lines might reflect a difference in the activity of cell surface proteases among the cell lines. Alternatively, the production of the transmembrane form of heregulin in DiFi-HRG4 cells might exceed the capacity of such proteases. To investigate the mechanism responsible for cetuximab resistance in DiFi-HRG cells, we examined differences in signal transduction between these cells and DiFi-Mock1 cells. In DiFi-Mock1 cells, cetuximab inhibited the phosphorylation of EGFR, HER2, HER3, AKT, and ERK as well as up-regulated BIM expression and down-regulated survivin expression, resulting in the induction of apoptosis. By contrast, in DiFi-HRG cell lines, whereas cetuximab inhibited EGFR and ERK phosphorylation, leading to BIM induction, it did not affect HER2, HER3, or AKT phosphorylation or survivin expression. Given that down-regulation both of AKT signaling and of the expression of its downstream target survivin is required for apoptosis induced by inhibition of receptor tyrosine kinases [14–16], our data suggest that sustained AKT-survivin signaling in the presence of cetuximab is responsible for the resistance of DiFi-HRG cell lines to this drug. To investigate further the relation between AKT signaling and the operation of a heregulin autocrine loop, we examined the effects of patritumab, a neutralizing monoclonal antibody to HER3, in DiFi-HRG4 cells. We found that exposure of these cells to patritumab in combination with cetuximab resulted in inhibition of EGFR, HER2, HER3, AKT, and ERK phosphorylation as well as in both up-regulation of BIM expression and down-regulation of survivin expression, leading to the induction of apoptosis. These results indicate that AKT signaling is triggered by heregulin binding to HER3.

Given that HER3 (a kinase-dead receptor) manifests impaired kinase activity [21], it requires dimerization with other HER family members to activate signaling after ligand binding [22, 23]. HER2 has been implicated as a dimerization partner of HER3, and heregulin stabilizes the HER2-HER3 heterodimer [9]. In this context, we examined the effects of lapatinib, a TKI for EGFR and HER2, in DiFi-HRG4 cells. Inhibition of EGFR and HER2 by lapatinib resulted in down-regulation of HER3, AKT, and ERK phosphorylation as well as in the induction of BIM and suppression of survivin expression in these cells, thereby triggering apoptosis (Supplementary Fig. S1A, S1B). These

findings suggest that, in DiFi-HRG cells, HER3 is trans-phosphorylated by HER2 as a result of heregulin-induced HER2-HER3 heterodimerization, which in turn leads to the activation of AKT signaling [24] (Fig. 5A, 5B, 5C). The heterodimerization partner of HER3 is thus likely switched from EGFR to HER2 as a result of the overexpression of heregulin in DiFi-HRG cells. We also found that patritumab alone inhibited the phosphorylation of HER3 and AKT as well as down-regulated survivin expression in DiFi-HRG4 cells but not in DiFi-Mock1 cells (Fig. 3D, 3E). These results suggest that patritumab may prevent ligand-dependent HER3 phosphorylation by blocking HER2-HER3 heterodimerization, whereas it has little effect on ligand-independent HER3 phosphorylation.

In our DiFi-HRG xenograft model, we showed that combination therapy with patritumab and cetuximab inhibited tumor growth to the same extent as did cetuximab alone in the DiFi-Mock1 xenograft model. Antagonism of the heregulin-HER3 interaction by patritumab thus represents an effective strategy to abrogate cetuximab resistance induced by heregulin derived from tumor cells. Given that elevated circulating levels of heregulin are associated with both de novo and acquired cetuximab resistance in mCRC patients [8], our model systems based on stable overexpression of heregulin are clinically relevant and should prove useful for establishing strategies to overcome cetuximab resistance mediated by the heregulin autocrine loop. Indeed, a recent phase I/II study with refractory colorectal cancer patients revealed potential antitumor activity of the combination of cetuximab and pertuzumab, a HER2-targeted antibody that blocks ligand-dependent HER2-HER3 heterodimerization. However, this drug combination was not tolerable as a result of overlapping toxicities [25]. Given that the toxicity profile of patritumab differs from that of pertuzumab [26], the combination of cetuximab and patritumab warrants evaluation in the clinical setting. We also found that the IC_{50} value for the antiproliferative effect of the combination of cetuximab and patritumab in DiFi-HRG4 cells was ~10 times as high as that for cetuximab alone in DiFi-Mock1 cells (Fig. 1C, Fig. 3A). The discrepancy between these *in vitro* data and our *in vivo* findings may suggest that antibody-dependent cellular cytotoxicity [27] involving NK cell activation plays a role in tumor growth inhibition by the combination of both agents. Moreover, combination therapy with these two IgG1 antibodies may result in an enhanced antitumor activity mediated by cytotoxic T lymphocytes [28] in the clinical setting. Given the recent evidence implicating the importance of interactions between therapeutic antibodies and the immune system in the efficacy of antibody treatment [20], further investigation of such mechanisms is warranted.

In conclusion, we have shown that consecutive activation of HER2-HER3 and AKT by heregulin in an autocrine-dependent manner confers resistance to cetuximab, and that patritumab restores cetuximab sensitivity in tumors with heregulin-induced cetuximab resistance. Further studies of combination therapy with patritumab and cetuximab are thus warranted in mCRC patients with heregulin-induced resistance to EGFR-targeted antibodies.

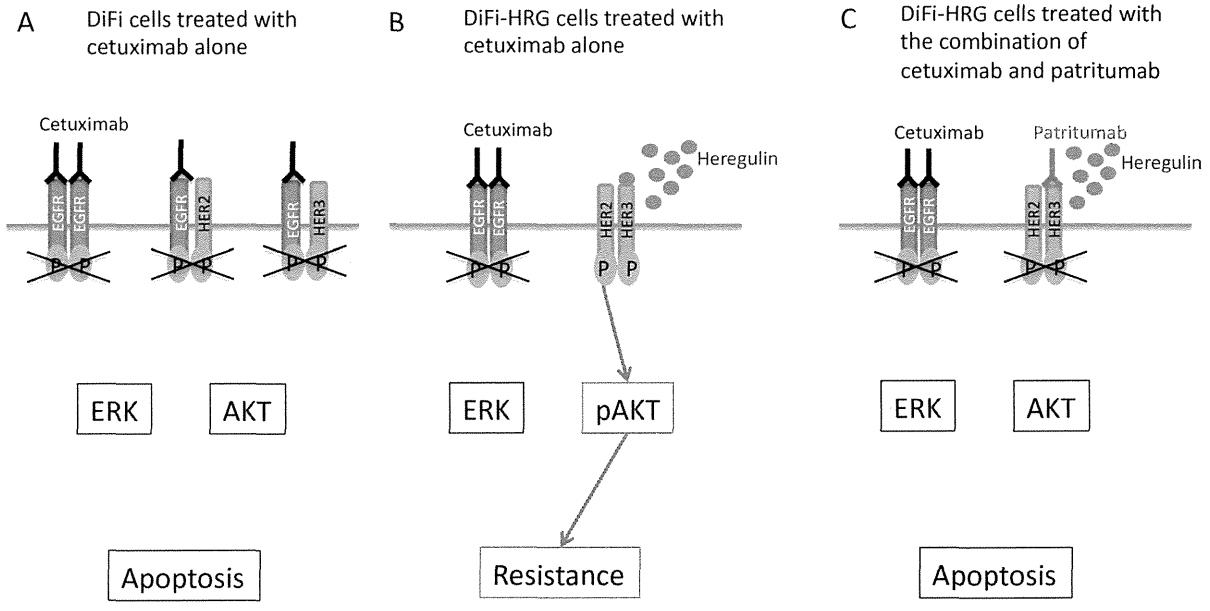

Figure 5: Model for intracellular signaling underlying the induction of apoptosis by cetuximab and patritumab in colorectal cancer cells. **(A)** DiFi colorectal cancer cells treated with cetuximab alone. **(B)** DiFi cells that stably overexpress heregulin (DiFi-HRG cells) are resistant to cetuximab as a result of HER2-HER3 heterodimerization and AKT activation induced by heregulin. **(C)** Patritumab abrogates cetuximab resistance mediated by the heregulin autocrine loop in DiFi-HRG cells.

MATERIALS AND METHODS

Cells and reagents

The DiFi human colorectal cancer cell line was kindly provided by P. A. Janne (Dana Farber Cancer Institute). DiFi cells were maintained under a humidified atmosphere of 5% CO_2 in air at 37°C in Dulbecco's modified Eagle's medium (DMEM) containing high glucose and supplemented with Ham's F-12 and 10% fetal bovine serum (FBS). Cetuximab was obtained from Merck Serono, and patritumab was kindly provided by Daiichi-Sankyo (Tokyo, Japan). Recombinant human heregulin (NRG1-β1/HRG1-β1 extracellular domain) was obtained from R&D Systems.

Establishment of cells stably overexpressing heregulin

A full-length cDNA encoding human heregulin (NRG1, GenBank accession no. NM_013956) was obtained from Origene (Rockville, MD). The amplification product was verified by sequencing after its cloning into the pCR-Blunt II-TOPO vector (Invitrogen). The heregulin cDNA was then excised from pCR-Blunt II-TOPO and transferred to the pQCXIH retroviral vector (Clontech), and retroviruses encoding heregulin were produced and used to infect DiFi cells as described [29]. Cells stably expressing heregulin were then isolated by selection with hygromycin (Invivogen) at 500 μg/mL.

Cell growth inhibition assay

Cells were transferred to 96-well flat-bottomed plates and cultured for 24 h before exposure to various concentrations of cetuximab or patritumab in medium containing 1% FBS for 120 h. Cell Counting Kit-8 solution (Dojindo, Kumamoto, Japan) was then added to each well, and the cells were incubated for 3 h at 37°C before measurement of absorbance at 490 nm with a Multiskan Spectrum instrument (Thermo Labsystems). Absorbance values were expressed as a percentage of that for nontreated cells, and the IC_{50} of cetuximab for inhibition of cell growth was determined.

Heregulin ELISA

The concentration of heregulin in cell culture supernatants was measured with the use of a sandwich ELISA (NRG1-β1 DuoSet, R&D Systems) as previously described [30]. Cells were seeded in six-well plates at a density of 0.5×10^6 cells per well in DMEM supplemented with 10% FBS. After the cells had achieved confluence, the medium was replaced with 5 ml of DMEM supplemented with 0.1% FBS, the cells were incubated for 48 h, and the culture supernatants were collected for assay of heregulin.

Immunoblot analysis

Cells were washed twice with ice-cold phosphate-buffered saline (PBS) and then lysed with 1 × Cell Lysis Buffer (Cell Signaling Technology) consisting of 20 mmol/L Tris-HCl (pH 7.5), 150 mmol/L NaCl, 1 mmol/L EDTA (disodium salt), 1 mmol/L EGTA, 1% Triton X-100, 2.5 mmol/L sodium pyrophosphate, 1 mmol/L β-glycerophosphate, 1 mmol/L Na_3VO_4, leupeptin (1 μg/mL), and 1 mmol/L phenylmethylsulfonyl fluoride. The protein concentration of the lysates was determined with a bicinchoninic acid assay kit (Thermo Fisher Scientific), and equal amounts of protein were subjected to SDS-polyacrylamide gel electrophoresis on a 7.5% gel (Bio-Rad). The separated proteins were transferred to a nitrocellulose membrane, which was then incubated with Blocking One solution (Nacalai Tesque) for 20 min at room temperature before incubation overnight at 4°C with primary antibodies. Antibodies to heregulin (NRG1-β1), to phosphorylated EGFR (phospho-Tyr^{1068}), to phosphorylated HER2 (phospho-Tyr^{1248}), to phosphorylated HER3 (phospho-Tyr^{1289}), to phosphorylated or total forms of AKT, to phosphorylated ERK, to PARP, and to BIM were obtained from Cell Signaling Technology; those to total HER3, to total ERK, and to survivin were from Santa Cruz Biotechnology; those to total EGFR were from Zymed/Invitrogen; those to total HER2 were from Millipore; and those to β-actin were from Sigma. The membrane was then washed with PBS containing 0.05% Tween 20 before incubation for 1 h at room temperature with horseradish peroxidase–conjugated secondary antibodies (GE Healthcare). Immune complexes were finally detected with ECL detection reagents (GE Healthcare).

Annexin V binding assay

The binding of annexin V to cells was measured with the use of an Annexin-V-FLUOS Staining Kit (Roche). Cells were harvested by exposure to trypsin-EDTA, washed with PBS, and centrifuged at 200 × *g* for 5 min. The cell pellets were resuspended in 100 μL of Annexin-V-FLUOS labeling solution, incubated for 10 to 15 min at 15° to 25°C, and then analyzed for fluorescence with a flow cytometer (FACSCalibur) and Cell Quest software (Becton Dickinson).

Tumor growth inhibition assay *in vivo*

All animal experiments were performed in accordance with the Recommendations for Handling of Laboratory Animals for Biomedical Research compiled by the Committee on Safety and Ethical Handling Regulations for Laboratory Animal Experiments, Kinki University. The ethical procedures followed conformed to the UKCCCR guidelines for the welfare and use of

animals in cancer research [31]. The study was also reviewed and approved by the Animal Ethics Committee of Kinki University (approval no. KAME-22-018). Cells were injected subcutaneously into the axilla of 5- to 6-week-old female athymic nude mice (BALB/c nu/nu; CLEA Japan), and treatment was initiated when tumors in each group of six mice achieved an average volume of 1000 to 1200 mm^3. Treatment groups consisted of vehicle control, cetuximab (1.0 mg/body), patritumab (1.0 mg/body), and the combination of both agents. Cetuximab and patritumab were administered by intraperitoneal injection twice a week for 4 weeks, with control animals receiving a 0.5% (w/v) aqueous solution of hydroxyl propylmethyl cellulose as vehicle. Tumor volume was determined from caliper measurements of tumor length (L) and width (W) according to the formula $LW^2/2$. Both tumor size and body weight were measured twice weekly. For ethical reasons, animals were removed from the study if the tumor volume exceeded 2500 mm^3.

Statistical analysis

Quantitative data are presented as means ± SE unless indicated otherwise. The significance of differences was evaluated with the unpaired two-tailed Student's t test. A P value of < 0.05 was considered statistically significant.

Conflict of interest statement

The authors declare no conflict of interest.

REFERENCES

1. Van Cutsem E, Kohne CH, Hitre E, Zaluski J, Chang Chien CR, Makhson A, D'Haens G, Pinter T, Lim R, Bodoky G, Roh JK, Folprecht G, Ruff P, Stroh C, Tejpar S, Schlichting M, et al. Cetuximab and chemotherapy as initial treatment for metastatic colorectal cancer. N Engl J Med. 2009; 360:1408–1417.
2. Bokemeyer C, Bondarenko I, Makhson A, Hartmann JT, Aparicio J, de Braud F, Donea S, Ludwig H, Schuch G, Stroh C, Loos AH, Zubel A, Koralewski P. Fluorouracil, leucovorin, and oxaliplatin with and without cetuximab in the first-line treatment of metastatic colorectal cancer. J Clin Oncol. 2009; 27:663–671.
3. Tol J, Koopman M, Cats A, Rodenburg CJ, Creemers GJ, Schrama JG, Erdkamp FL, Vos AH, van Groeningen CJ, Sinnige HA, Richel DJ, Voest EE, Dijkstra JR, Vink-Borger ME, Antonini NF, Mol L, et al. Chemotherapy, bevacizumab, and cetuximab in metastatic colorectal cancer. N Engl J Med. 2009; 360:563–572.
4. Di Nicolantonio F, Martini M, Molinari F, Sartore-Bianchi A, Arena S, Saletti P, De Dosso S, Mazzucchelli L, Frattini M, Siena S, Bardelli A. Wild-type BRAF is required for response to panitumumab or cetuximab in metastatic colorectal cancer. J Clin Oncol. 2008; 26:5705–5712.
5. Montagut C, Dalmases A, Bellosillo B, Crespo M, Pairet S, Iglesias M, Salido M, Gallen M, Marsters S, Tsai SP, Minoche A, Seshagiri S, Serrano S, Himmelbauer H, Bellmunt J, Rovira A, et al. Identification of a mutation in the extracellular domain of the Epidermal Growth Factor Receptor conferring cetuximab resistance in colorectal cancer. Nat Med. 2012; 18:221–223.
6. Misale S, Yaeger R, Hobor S, Scala E, Janakiraman M, Liska D, Valtorta E, Schiavo R, Buscarino M, Siravegna G, Bencardino K, Cercek A, Chen CT, Veronese S, Zanon C, Sartore-Bianchi A, et al. Emergence of KRAS mutations and acquired resistance to anti-EGFR therapy in colorectal cancer. Nature. 2012; 486:532–536.
7. Bardelli A, Corso S, Bertotti A, Hobor S, Valtorta E, Siravegna G, Sartore-Bianchi A, Scala E, Cassingena A, Zecchin D, Apicella M, Migliardi G, Galimi F, Lauricella C, Zanon C, Perera T, et al. Amplification of the MET receptor drives resistance to anti-EGFR therapies in colorectal cancer. Cancer Discov. 2013; 3:658–673.
8. Yonesaka K, Zejnullahu K, Okamoto I, Satoh T, Cappuzzo F, Souglakos J, Ercan D, Rogers A, Roncalli M, Takeda M, Fujisaka Y, Philips J, Shimizu T, Maenishi O, Cho Y, Sun J, et al. Activation of ERBB2 signaling causes resistance to the EGFR-directed therapeutic antibody cetuximab. Sci Transl Med. 2011; 3:99ra86.
9. Wallasch C, Weiss FU, Niederfellner G, Jallal B, Issing W, Ullrich A. Heregulin-dependent regulation of HER2/neu oncogenic signaling by heterodimerization with HER3. EMBO J. 1995; 14:4267–4275.
10. Gala K, Chandarlapaty S. Molecular pathways: HER3 targeted therapy. Clin Cancer Res. 2014; 20:1410–1416.
11. Freeman D, Ogbagabreiel S, Rothe M, Radinsky R, Treder M. 2008; Fully human Anti-HER3 monoclonal antibodies (mAbs) have unique *in vitro* and *in vivo* functional and antitumor activities versus other HER family inhibitors (abstract). Proceedings of the Annual Meeting of the American Association for Cancer Research; San Diego, CA: AACR.
12. Treder M, Hartmann S, Ogbagabrei S, Borges E, Green L, Kang Jea (2008); Fully human Anti-HER3 monoclonal antibodies (mAbs) inhibit oncogenic signaling and tumor cell growth *in vitro* and vivo. Proceedings of the Annual Meeting of the American Association for Cancer Research; San Diego, CA.: AACR.
13. McDermott U, Sharma SV, Dowell L, Greninger P, Montagut C, Lamb J, Archibald H, Raudales R, Tam A, Lee D, Rothenberg SM, Supko JG, Sordella R, Ulkus LE, Iafrate AJ, Maheswaran S, et al. Identification of genotype-correlated sensitivity to selective kinase inhibitors by using high-throughput tumor cell line profiling. Proc Natl Acad Sci U S A. 2007; 104:19936–19941.
14. Okamoto K, Okamoto I, Okamoto W, Tanaka K, Takezawa K, Kuwata K, Yamaguchi H, Nishio K,

Nakagawa K. Role of survivin in EGFR inhibitor-induced apoptosis in non-small cell lung cancers positive for EGFR mutations. Cancer Res. 2010; 70:10402–10410.

15. Tanizaki J, Okamoto I, Fumita S, Okamoto W, Nishio K, Nakagawa K. Roles of BIM induction and survivin downregulation in lapatinib-induced apoptosis in breast cancer cells with HER2 amplification. Oncogene. 2011; 30:4097–4106.
16. Okamoto W, Okamoto I, Arao T, Kuwata K, Hatashita E, Yamaguchi H, Sakai K, Yanagihara K, Nishio K, Nakagawa K. Antitumor action of the MET tyrosine kinase inhibitor crizotinib (PF-02341066) in gastric cancer positive for MET amplification. Mol Cancer Ther. 2012; 11:1557–1564.
17. Siena S, Sartore-Bianchi A, Di Nicolantonio F, Balfour J, Bardelli A. Biomarkers predicting clinical outcome of epidermal growth factor receptor-targeted therapy in metastatic colorectal cancer. J Natl Cancer Inst. 2009; 101:1308–1324.
18. De Roock W, De Vriendt V, Normanno N, Ciardiello F, Tejpar S. KRAS, BRAF, PIK3CA, and PTEN mutations: implications for targeted therapies in metastatic colorectal cancer. Lancet Oncol. 2011; 12:594–603.
19. Bardelli A, Siena S. Molecular mechanisms of resistance to cetuximab and panitumumab in colorectal cancer. J Clin Oncol. 2010; 28:1254–1261.
20. Troiani T, Zappavigna S, Martinelli E, Addeo SR, Stiuso P, Ciardiello F, Caraglia M. Optimizing treatment of metastatic colorectal cancer patients with anti-EGFR antibodies: overcoming the mechanisms of cancer cell resistance. Expert Opin Biol Ther. 2013; 13:241–255.
21. Guy PM, Platko JV, Cantley LC, Cerione RA, Carraway KL, 3rd . Insect cell-expressed p180erbB3 possesses an impaired tyrosine kinase activity. Proc Natl Acad Sci U S A. 1994; 91:8132–8136.
22. Holbro T, Beerli RR, Maurer F, Koziczak M, Barbas CF, 3rd, Hynes NE. The ErbB2/ErbB3 heterodimer functions as an oncogenic unit: ErbB2 requires ErbB3 to drive breast tumor cell proliferation. Proc Natl Acad Sci U S A. 2003; 100:8933–8938.
23. Knowlden JM, Hutcheson IR, Jones HE, Madden T, Gee JM, Harper ME, Barrow D, Wakeling AE, Nicholson RI. Elevated levels of epidermal growth factor receptor/c-erbB2 heterodimers mediate an autocrine growth regulatory pathway in tamoxifen-resistant MCF-7 cells. Endocrinology. 2003; 144:1032–1044.
24. Tzahar E, Waterman H, Chen X, Levkowitz G, Karunagaran D, Lavi S, Ratzkin BJ, Yarden Y. A hierarchical network of interreceptor interactions determines signal transduction by Neu differentiation factor/neuregulin and epidermal growth factor. Mol Cell Biol. 1996; 16:5276–5287.
25. Rubinson DA, Hochster HS, Ryan DP, Wolpin BM, McCleary NJ, Abrams TA, Chan JA, Iqbal S, Lenz HJ, Lim D, Rose J, Bekaii-Saab T, Chen HX, Fuchs CS, Ng K. Multi-drug inhibition of the HER pathway in metastatic colorectal cancer: results of a phase I study of pertuzumab plus cetuximab in cetuximab-refractory patients. Invest New Drugs. 2014; 32:113–122.
26. LoRusso P, Janne PA, Oliveira M, Rizvi N, Malburg L, Keedy V, Yee L, Copigneaux C, Hettmann T, Wu CY, Ang A, Halim AB, Beckman RA, Beaupre D, Berlin J. Phase I Study of U3-1287, a Fully Human Anti-HER3 Monoclonal Antibody, in Patients with Advanced Solid Tumors. Clin Cancer Res. 2013; 19:3078–3087.
27. Kimura H, Sakai K, Arao T, Shimoyama T, Tamura T, Nishio K. Antibody-dependent cellular cytotoxicity of cetuximab against tumor cells with wild-type or mutant epidermal growth factor receptor. Cancer Sci. 2007; 98:1275–1280.
28. Correale P, Botta C, Cusi MG, Del Vecchio MT, De Santi MM, Gori Savellini G, Bestoso E, Apollinari S, Mannucci S, Marra M, Abbruzzese A, Aquino A, Turriziani M, Bonmassar L, Caraglia M, Tagliaferri P. Cetuximab +/– chemotherapy enhances dendritic cell-mediated phagocytosis of colon cancer cells and ignites a highly efficient colon cancer antigen-specific cytotoxic T-cell response *in vitro*. Int J Cancer. 2012; 130:1577–1589.
29. Tanaka K, Arao T, Maegawa M, Matsumoto K, Kaneda H, Kudo K, Fujita Y, Yokote H, Yanagihara K, Yamada Y, Okamoto I, Nakagawa K, Nishio K. SRPX2 is overexpressed in gastric cancer and promotes cellular migration and adhesion. Int J Cancer. 2009; 124:1072–1080.
30. Yonesaka K, Zejnullahu K, Lindeman N, Homes AJ, Jackman DM, Zhao F, Rogers AM, Johnson BE, Janne PA. Autocrine production of amphiregulin predicts sensitivity to both gefitinib and cetuximab in EGFR wild-type cancers. Clin Cancer Res. 2008; 14:6963–6973.
31. Workman P, Aboagye EO, Balkwill F, Balmain A, Bruder G, Chaplin DJ, Double JA, Everitt J, Farningham DA, Glennie MJ, Kelland LR, Robinson V, Stratford IJ, Tozer GM, Watson S, Wedge SR, et al. Guidelines for the welfare and use of animals in cancer research. Br J Cancer. 2010; 102:1555–1577.

Tolerability of Nintedanib (BIBF 1120) in Combination with Docetaxel: A Phase 1 Study in Japanese Patients with Previously Treated Non–Small-Cell Lung Cancer

Isamu Okamoto, MD, PhD,† Masaki Miyazaki, MD, PhD,*‡ Masayuki Takeda, MD, PhD,* Masaaki Terashima, MD, PhD,*§ Koichi Azuma, MD, PhD,*‖ Hidetoshi Hayashi, MD, PhD,*¶ Hiroyasu Kaneda, MD, PhD,* Takayasu Kurata, MD, PhD,*# Junji Tsurutani, MD, PhD,* Takashi Seto, MD, PhD,** Fumihiko Hirai, MD, PhD,** Koichi Konishi, BPharm,†† Akiko Sarashina, MSc,‡‡ Nobutaka Yagi, MSc,†† Rolf Kaiser, MD,§§ and Kazuhiko Nakagawa, MD, PhD**

Background: This phase I, open-label study evaluated the safety/tolerability and maximum tolerated dose of second-line nintedanib combined with docetaxel in Japanese patients with advanced non–small-cell lung cancer.

Methods: Eligible patients received docetaxel 60 or 75 mg/m^2 (day 1) plus nintedanib 100, 150, or 200 mg twice daily (bid; days 2–21) in 21-day cycles. Standard 3 + 3 dose escalations were performed separately in patient cohorts with a body surface area (BSA) of less than 1.5 m^2 (BSA <1.5) and BSA greater than or equal to 1.5, respectively.

Results: Forty-two patients (17 BSA <1.5, 25 BSA ≥1.5) were treated. The maximum tolerated dose of nintedanib was 150 and 200 mg bid in patients with BSA less than 1.5 and BSA greater than or equal to 1.5 (BSA ≥1.5), respectively, in combination with 75 mg/m^2 of docetaxel. Dose-limiting toxicities (all grade 3 hepatic enzyme elevations) occurred in 12 patients (six per cohort). Drug-related adverse events included neutropenia (95%), leukopenia (83%), fatigue (76%), alopecia (71%), decreased appetite (67%), and elevations in alanine aminotransferase (64%) and aspartate aminotransferase (64%). All hepatic enzyme elevations were reversible and manageable with dose reduction or discontinuation. Among 38 evaluable patients, 10 (26%) had a partial response and 18 (47%) had stable disease.

Conclusion: Continuous treatment with second-line nintedanib combined with docetaxel was manageable and showed promising signs of efficacy in Japanese patients with advanced non–small-cell lung cancer.

Key Words: Clinical trials, Phase I, Docetaxel, Japanese, Nintedanib, Non–small-cell lung cancer, Pharmacokinetics.

(*J Thorac Oncol.* 2015;10: 346–352)

Few treatment options are available for patients with advanced non–small-cell lung cancer (NSCLC) who fail first-line chemotherapy. Currently, the only licensed second-line therapies for individuals with NSCLC, who do not harbor identifiable driver oncogenes, such as sensitizing epidermal growth factor receptor (*EGFR*) gene mutations or anaplastic lymphoma kinase (*ALK*) gene translocations, are docetaxel, gemcitabine, pemetrexed (for nonsquamous NSCLC), and erlotinib.[1] Although these treatments are efficacious, survival benefits are modest. Hence, there is an urgent need for effective and well-tolerated second-line options.

Angiogenesis plays an important role in the development and differentiation of NSCLC.[2] Targeting vascular endothelial growth factor (VEGF) signaling appears to be particularly important in advanced NSCLC, given the proven efficacy of the VEGF-targeted monoclonal antibody bevacizumab as first-line therapy in large-scale trials.[3,4] However, to date no oral tyrosine kinase inhibitors of VEGF receptors have been approved for the treatment of advanced NSCLC. Mechanisms that support solid tumor angiogenesis include VEGF, fibroblast growth factor, and platelet-derived growth factor signaling pathways.[5–8] Nintedanib (BIBF 1120) is a potent, oral, small-molecule triple angiokinase inhibitor that targets VEGF receptors 1 to 3, platelet-derived growth factor

*Department of Medical Oncology, Kinki University Faculty of Medicine, Osaka, Japan; †Center for Clinical and Translational Research, Faculty of Medicine, Kyusyu University Hospital, Fukuoka, Japan; ‡Department of Internal Medicine, Suita Municipal Hospital, Osaka, Japan; §Department of Medical Oncology, Nara Hospital, Kinki University Faculty of Medicine, Nara, Japan; ‖Department of Medicine, Division of Respirology, Neurology, and Rheumatology, Kurume University Hospital, Fukuoka, Japan; ¶Department of Medical Oncology, Kishiwada Municipal Hospital, Osaka, Japan; #Department of Thoracic Oncology, Kansai Medical University, Hirakata Hospital, Osaka, Japan; **Department of Medical Oncology, National Kyushu Cancer Centre, Fukuoka, Japan; ††Department of Medical Oncology, National Kyushu Cancer Centre, Fukuoka, Japan; ‡‡Nippon Boehringer Ingelheim Co. Ltd., Medical Development Division, Hyogo, Japan; and §§Clinical Pharmacokinetics/Pharmacodynamics Department, Boehringer Ingelheim Pharma GmbH & Co. KG, Biberach, Germany.

Funding: This work was supported by Boehringer Ingelheim.

K.K., A.S., and N.Y. are employees of Nippon Boehringer Ingelheim Co. Ltd.; R.K. is an employee of Boehringer Ingelheim Pharma GmbH & Co.; T.S. has received honoraria from Boehringer Ingelheim and is a member of their speaker bureau; all remaining authors have declared no conflict of interest.

Address for correspondence: Isamu Okamoto, MD, PhD, Center for Clinical and Translational Research, Kyushu University Hospital, 3-1-1 Maidashi, Higashiku, Fukuoka 812-8582, Japan. E-mail: okamotoi@kokyu.med.kyushu-u.ac.jp

DOI: 10.1097/JTO.0000000000000395

ISSN: 1556-0864/15/1002-0346

receptors alpha and beta, and fibroblast growth factor receptors 1 to 3, besides RET and Flt3.[9] Preclinical experiments have shown that nintedanib can delay tumor growth and inhibit angiogenesis in various xenograft models of human cancer, including NSCLC.[9] More recently, the global LUME-Lung 1 phase III trial (Study 1199.13; NCT00805194) for previously treated advanced NSCLC demonstrated that treatment with a combination of nintedanib and docetaxel produced a significant and clinically meaningful improvement in overall survival compared with docetaxel and placebo in predefined patients with adenocarcinoma tumor histology.[10]

In a recent Japanese phase I study, the maximum tolerated dose (MTD) of nintedanib monotherapy was 200 mg bid, which is lower than the MTD of 250 mg bid for Caucasian patients.[11,12] Although the reason for this difference remains unclear, analogous differences in the tolerability of chemotherapy for advanced NSCLC between Japanese and US patients have been reported previously, and have been related to differences in genotypic variants between the two populations.[13] In addition, the standard dose of docetaxel 60 mg/m^2 commonly employed for Japanese patients with advanced NSCLC[14] is lower than the 75 mg/m^2 dose used for Western populations.[10,15] This phase I dose-escalation study (Study 1199.29; NCT00876460) was conducted to define the MTD of nintedanib combined with docetaxel, and to confirm the safety/tolerability profile of the combination in Japanese patients with advanced NSCLC following failure of first-line platinum-based chemotherapy.

PATIENTS AND METHODS

Study Population

Patients aged 20 to 74 years with histologically or cytologically confirmed, advanced stages IIIB to IV or recurrent NSCLC (any histology) who had received one platinum-based chemotherapy regimen (not containing docetaxel) were enrolled. Patients had an Eastern Cooperative Oncology Group performance status of 0 to 1, a life expectancy exceeding 3 months, and adequate organ function. Exclusion criteria included: active brain metastases; gastrointestinal disorders that could interfere with the absorption of the study drug; history of major thrombotic or clinically relevant major bleeding event in the past 6 months; clinically significant hemoptysis in the past 3 months; active multiple primary neoplasms; or significant cardiovascular disease.

Study Design

This open-label trial utilized a standard 3 + 3 dose-escalation design. Eligible patients received intravenous docetaxel at a dose of 60 mg/m^2 or 75 mg/m^2 on day 1, followed by continuous, oral nintedanib bid on days 2 to 21 in 21-day cycles. Nintedanib was started at a dose of 100 mg bid and escalated up to 200 mg bid in 50 mg bid intervals. Continuous nintedanib monotherapy was permitted in cases where docetaxel had to be permanently discontinued for reasons other than progression, and the patient had already received at least four treatment cycles of combination therapy.

Dose-limiting toxicity (DLT) was defined as nonhematologic toxicity greater than Common Terminology Criteria for Adverse Events (CTCAE) grade 3, excluding electrolyte abnormalities or isolated elevations of γ-glutamyl transpeptidase (γ-GT); grade 3 or higher gastrointestinal toxicity or hypertension despite optimal supportive care/intervention; grade 4 neutropenia for more than 7 days despite optimal supportive care; grade 4 febrile neutropenia of any duration; grade 2 or higher alanine aminotransferase (ALT) and/or aspartate aminotransferase (AST) elevations combined with grade 2 or higher bilirubin elevations; inability to resume nintedanib dosing within 14 days of stopping treatment due to treatment-related toxicity. DLTs observed in the first 21 days of treatment were used to determine MTD, defined as the highest dose at which incidence of DLTs in cycle 1 was less than or equal to 33.3%.

After testing nintedanib 100 mg bid plus docetaxel 60 mg/m^2 (N100/D60), nintedanib 150 mg bid plus docetaxel 60 mg/m^2 (N150/D60), and nintedanib 200 mg bid plus docetaxel 60 mg/m^2 (N200/D60) without considering body surface area (BSA), dose escalations were performed separately in two patient cohorts with a BSA of less than 1.5 m^2 (BSA <1.5) and greater than or equal to 1.5 m^2 (BSA ≥1.5), respectively. This protocol amendment was recommended by the external Efficacy and Safety Review Committee following early observation of a high incidence of DLTs in patients with a BSA of less than 1.5 m^2.

The institutional review board reviewed and approved the protocol and its amendments. The trial was conducted in compliance with the study protocol, the Declaration of Helsinki, and Good Clinical Practice guidelines. All patients provided written informed consent.

Assessments

Adverse events (AEs) were assessed according to CTCAE version 3.0 throughout the trial and for 28 days after treatment cessation. All safety analyses were undertaken in patients who had received 1 dose or more of nintedanib. Objective tumor response was evaluated according to the Response Evaluation Criteria in Solid Tumors (RECIST 1.0). Tumor assessment was performed at screening and every 6 weeks on day 1 (within 7 days) of each odd-numbered treatment cycle (cycles 3, 5, etc.). Hematology and biochemistry assessments were undertaken at screening and at predefined intervals during the trial.

To investigate the possible effect of nintedanib on the pharmacokinetics (PK) of docetaxel, blood samples were taken predose and 1, 1.5, 2, 3, 4, 7, 24, and 48 hours postdose on days 1 to 3 of cycles 1 and 2. Sampling for PK characterization of nintedanib was carried out on days 2 to 3 of cycle 1, with samples taken predose, 1, 2, 3, 4, 6, 7, 10, and 24 hours after the morning dose. Samples for evaluation of trough concentrations of nintedanib were taken on days 8 and 15 of the first two cycles, and on days 1 to 3 during cycle 2, before the morning dose. All PK analyses were carried out using WinNonlin software, applying a noncompartmental approach.

Statistical Analysis

The primary end points were the determination of the MTD of nintedanib in combination with docetaxel at doses

of 60 or 75 mg/m^2, and the assessment of the frequency and severity of AEs. Secondary end points included PKs of nintedanib and docetaxel, best tumor response and progression-free survival (PFS). Descriptive statistics are presented.

RESULTS

Patients

A total of 43 patients with advanced NSCLC were enrolled into this study from March 2009 to August 2012. One patient discontinued due to a non-DLT adverse event before the first dose of nintedanib was administered and was excluded from the study. Baseline characteristics, except for gender and clinical stage, were similar between the two BSA cohorts (Table 1).

At the time of the database lock (June 11, 2013), all 42 patients had discontinued combination treatment. Reasons for discontinuation included progressive disease (n = 22), AEs (n = 14), and withdrawal of consent (n = 3). Three patients continued to be treated with nintedanib monotherapy after discontinuation of docetaxel due to drug-related AEs (grade 1 and 2 peripheral neuropathy in two patients, and grade 2 pleural effusion in one patient). Median (range) number of days of treatment administered was 126.5 (7–1339).

Maximum Tolerated Dose and Dose-Limiting Toxicities

The allocation of patients to treatment during the study is summarized in Figure 1. Of the 42 patients who received nintedanib treatment, three patients were excluded from the DLT assessment due to low compliance with study treatment: one excluded patient had a non-DLT adverse event,

TABLE 1. Patient Characteristics at Baseline and Treatment Allocation

	Patients with BSA <1.5 m^2 (n = 17)	Patients with BSA ≥1.5 m^2 (n = 25)	All Patients (n = 42)
Age, years			
Median (range)	65 (45–72)	62 (47–73)	64 (45–73)
Gender, n (%)			
Male	6 (35)	23 (92)	29 (69)
Female	11 (65)	2 (8)	13 (31)
ECOG performance score, n (%)			
0	6 (35)	8 (32)	14 (33)
1	11 (65)	17 (68)	28 (67)
Clinical stage, n (%)			
IIIB	1 (6)	6 (24)	7 (17)
IV	16 (94)	19 (76)	35 (83)
Histology, n (%)			
Adenocarcinoma	14 (82)	19 (76)	33 (79)
Squamous cell carcinoma	3 (18)	5 (20)	8 (19)
Large-cell carcinoma	0	1 (4)	1 (2)

bid, twice daily; BSA, body surface area; D, docetaxel; DLT, dose-limiting toxicity; ECOG, Eastern Cooperative Oncology Group; N, nintedanib.

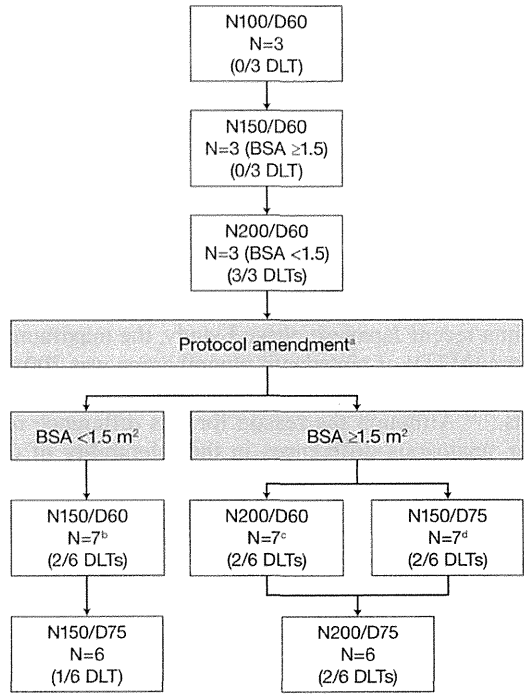

FIGURE 1. Patient flow. N100/D60, nintedanib 100 mg bid plus docetaxel 60 mg/m^2; N150/D60, nintedanib 150 mg bid plus docetaxel 60 mg/m^2; N150/D75, nintedanib 150 mg bid plus docetaxel 75 mg/m^2; N200/D60, nintedanib 200 mg bid plus docetaxel 60 mg/m^2; N200/D75, nintedanib 200 mg bid plus docetaxel 75 mg/m^2. [a]Protocol amendment by the Efficacy and Safety Review Committee, which recommended separate assessments of dose levels for patients with a body surface area (BSA) <1.5 m^2 and ≥1.5 m^2. [b]One patient was replaced due to low compliance with study drugs administration with a non-dose-limiting toxicity adverse event (pneumonia). [c]One patient was replaced due to insufficient data to evaluate the duration of grade 4 neutropenia as a dose-limiting toxicity. [d]One patient was replaced due to early withdrawal of consent.

the second patient withdrew consent before the completion of cycle 1, and there were insufficient data to confirm a DLT occurrence in the third patient. Three patients were enrolled in the N100/D60 cohort, three patients in the N150/D60 cohort, and three patients in the N200/D60 cohort, without consideration of their BSA. No DLT was observed for the first and second cohorts (N100/D60 and N150/D60). At 200 mg bid (N200/D60), all three patients experienced DLTs (ALT, AST, and γ-glutamytranferase increases in two patients, and ALT and AST increase in one patient) that were fully reversible (Table 2). All three patients who experienced DLTs at N200/D60 had BSA less than 1.5, whereas the three patients treated with N150/D60 who did not experience DLTs had BSA greater than or equal to 1.5. In a previous investigation of nintedanib monotherapy in Japanese patients,[11] all DLTs at 200 mg bid were observed in patients whose BSAs were smaller than those of patients without observed DLTs. The external Efficacy and Safety Review Committee recommended the protocol amendments for reassessment of

TABLE 2. Observed Dose-Limiting Toxicities in Treatment Cycle 1 at Each Nintedanib Dose Level Among Evaluable Patients with BSA <1.5 m^2 or BSA ≥1.5 m^2

Cohort	Nintedanib Dose (mg bid)	Docetaxel Dose (mg/m^2)	No. of DLTs/Patients[a]	Nature of DLT
—	100	60	0/3[b]	—
BSA <1.5m^2	150	60	2/6	(1) ALT and AST elevation; (2) ALT elevation
		75	1/6	(1) ALT and AST elevation
	200	60	3/3	(1) ALT, AST, and γ-GT elevation; (2) ALT, AST, and γ-GT elevation; (3) ALT and AST elevation
BSA ≥1.5m^2	150	60	0/3	—
		75	2/6	(1) ALT and γ-GT elevation; (2) ALT elevation
	200	60	2/6	(1) ALT, AST and γ-GT elevation; (2) ALT and γ-GT elevation
		75	2/6	(1) ALT, AST, and γ-GT elevation; (2) ALT elevation

[a]Patients eligible for evaluation of dose-limiting toxicity.
[b]BSA in 100 mg bid group: <1.5 m^2, $n = 1$; ≥1.5 m^2, $n = 2$.
ALT, alanine aminotransferase; AST, aspartate aminotransferase; bid, twice daily; BSA, body surface area; DLT, dose-limiting toxicity; γ-GT, gamma glutamyltransferase.

the N150/D60 dose in patients with BSA less than 1.5, and for subsequent dose escalations to be performed separately for cohorts with BSA less than 1.5 and BSA greater than or equal to 1.5, respectively.

As shown in Table 2, of 12 patients with BSA less than 1.5 treated in the N150/D60 or the nintedanib 150 mg bid plus docetaxel 75 mg/m^2 (N150/D75) cohorts, three patients experienced DLTs (liver enzyme elevations that were reversible with dose reduction or discontinuation); two in the N150/D60 cohort and one in the N150/D75 cohort. Of 12 patients with BSA greater than or equal to 1.5 treated in the N200/D60 and the nintedanib 200 mg bid plus docetaxel 75 mg/m^2 (N200/D75) cohorts, respectively, two of six patients in each cohort experienced DLTs (reversible liver enzyme elevations). In eight of 12 patients who developed DLTs, nintedanib was reintroduced with dose reduction following rapid recovery of liver enzyme levels; one patient required a second dose reduction (Fig. 2). The MTD of nintedanib was thus 150 and 200 mg bid combined with 75 mg/m^2 of docetaxel in the BSA less than 1.5 and BSA greater than or equal to 1.5 cohorts, respectively.

Safety Profile of Nintedanib

Of the 42 patients who received combination treatment, the most frequent drug-related AEs (all CTCAE grades) were neutropenia, leukopenia, fatigue, alopecia, decreased appetite, ALT/AST elevations, diarrhea, and γ-GT elevations (Table 3). The only grade 4 AEs were neutropenia ($n = 37$) and leukopenia ($n = 9$). Liver enzyme elevations were asymptomatic, and manageable with dose reduction or discontinuation. Among drug-related AEs commonly observed with other VEGF-targeted tyrosine kinase inhibitors, grade 1 or 2 rash was observed in 17 patients, grade 2 proteinuria in one patient, and grade 1 bleeding in seven patients; hypertension, perforation, and thromboembolism were not observed in this study.

Two patients died during the study period. One of these deaths occurred in a male patient (53 years of age; BSA = 1.92 m^2), who was previously treated concurrently with radiation to the mediastinum and systemic chemotherapy (vinorelbine plus cisplatin) until 19 months before beginning the present study treatment (N200/D60) for metastatic disease in mediastinal lymph nodes and an abdominal para-aortic lymph node. He responded to the study treatment

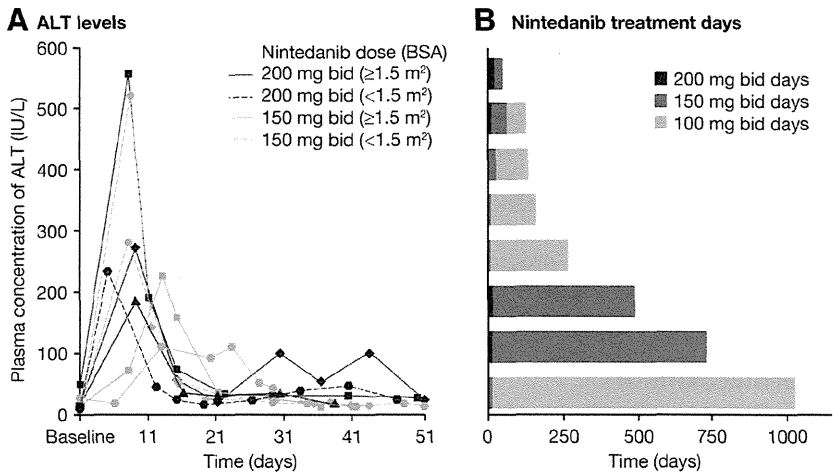

FIGURE 2. Change in alanine aminotransferase (ALT) values in all eight patients with dose reduction on nintedanib by dose-limiting toxicity (DLT) during first treatment course and nintedanib treatment days. BSA, body surface area.

ALT, alanine aminotransferase; bid, twice daily; DLT, dose-limiting toxicity

TABLE 3. Frequency of Patients with Drug-Related AEs (≥20% Incidence) Across all Dose Groups in all Treatment Courses by Body Surface Area

	Patients with BSA <1.5 m² (n = 17)		Patients with BSA ≥1.5 m² (n = 25)		All patients (n = 42)	
n (%)	CTCAE grade 3–4	All CTCAE grades	CTCAE grade 3–4	All CTCAE grades	CTCAE grade 3–4	All CTCAE grades
Hematologic						
Neutropenia	17 (100)	17 (100)	23 (92)	23 (92)	40 (95)	40 (95)
Leukopenia	10 (59)	14 (82)	17 (68)	21 (84)	27 (64)	35 (83)
Anemia	0	4 (24)	0	6 (24)	0	10 (24)
Nonhematologic						
Fatigue	0	15 (88)	0	17 (68)	0	32 (76)
Alopecia	0	12 (71)	0	18 (72)	0	30 (71)
Decreased appetite	1 (6)	13 (76)	0	15 (60)	1 (2)	28 (67)
Diarrhea	0	6 (35)	1 (4)	16 (64)	1 (2)	22 (52)
Dysgeusia	0	6 (35)	0	11 (44)	0	17 (40)
Rash	0	8 (47)	0	9 (36)	0	17 (40)
Nausea	0	7 (41)	0	8 (32)	0	15 (36)
Vomiting	0	9 (53)	0	5 (20)	0	14 (33)
Stomatitis	0	4 (23)	0	8 (32)	0	12 (29)
Peripheral sensory neuropathy	1 (6)	3 (18)	0	7 (28)	1 (2)	10 (24)
Edema	0	5 (29)	0	4 (16)	0	9 (21)
Laboratory abnormalities						
ALT increased	6 (35)	13 (76)	6 (24)	14 (56)	12 (29)	27 (64)
AST increased	5 (29)	13 (76)	2 (8)	14 (56)	7 (17)	27 (64)
γ-GT increased	3 (18)	10 (59)	4 (16)	12 (48)	7 (17)	22 (52)
ALP increased	1 (6)	9 (53)	0	9 (36)	1 (2)	18 (43)

ALP, alkaline phosphatase; ALT, alanine aminotransferase; AST, aspartate aminotransferase; BSA, body surface area; CTCAE, Common Terminology Criteria for Adverse Events; γ-GT, gamma glutamyltransferase.

(partial response), and the combination treatment was continued until cycle 27. Notable on-treatment AEs were grade 3 to 4 neutropenia and grade 1 fatigue, with no AEs of bleeding observed before the fatal event. On day 12 of cycle 27, the patient died with bleeding suggestive of hemoptysis. The second death occurred in a woman (69 years; BSA = 1.29 m²) who had progressed after first-line platinum-based chemotherapy, and received a total of three cycles of N150/D75 in the present study. On the planned day 1 of cycle 4, a grade 1 AST elevation was observed, docetaxel administration was postponed, and nintedanib treatment was interrupted. Eight days after nintedanib interruption, the study treatment was postponed again because of a grade 1 AST elevation despite no abnormalities in any other vital signs. Fourteen days after nintedanib interruption, the patient died. Based on the details available, the most probable reason for death for both patients was underlying advanced progressive lung cancer. However, the information was not sufficient to clarify the reasons for their events.

Pharmacokinetics

Despite interpatient variability, nintedanib AUC and C_{max} increased in an almost dose-proportional manner following single-dose administration (Supplemental Table S1, SDC 1, http://links.lww.com/JTO/A737). Plasma concentrations of nintedanib reached maximum levels 2 to 3 hours postadministration and then declined, with a half-life of 8 to 9 hours.

PK analysis revealed no apparent interactions between nintedanib and docetaxel. The AUC and C_{max} for nintedanib (non-dose-normalized) in this study were similar to those observed in a previous Japanese phase I study of single-agent nintedanib.[11] Similarly, coadministration of nintedanib did not affect docetaxel PKs (Supplemental Table S2, SDC 1, http://links.lww.com/JTO/A737; Supplemental Figure S1, SDC 2, http://links.lww.com/JTO/A738).

Dose-normalized PK parameters ($C_{max,norm}$, $AUC_{0\text{-}12,norm}$, and $AUC_{0\text{-}\infty,norm}$) were compared among patients with BSA less than 1.5 and BSA greater than or equal to 1.5 patients. Although geometric mean values of nintedanib $C_{max,norm}$, $AUC_{0\text{-}12,norm}$, and $AUC_{0\text{-}\infty,norm}$ were slightly higher in patients with BSA less than 1.5 than in patients with BSA greater than or equal to 1.5, the wide overlap of individual patient values indicated no significant differences in nintedanib exposure between the two patient cohorts (Figure 3).

Efficacy

Four of 42 patients were excluded from the efficacy evaluation for objective response according to RECIST because they had no post-treated tumor measurement due to treatment discontinuation during cycle 1; discontinuation

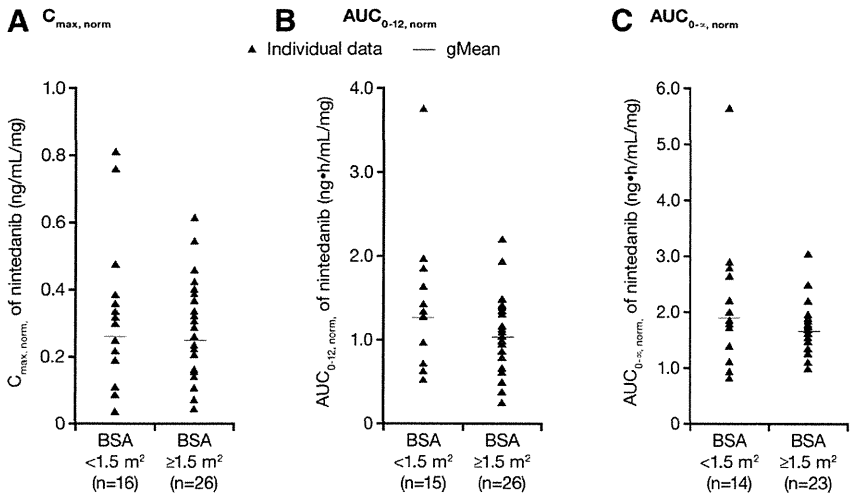

FIGURE 3. $C_{max, norm}$ (*A*), $AUC_{0-12, norm}$ (*B*), and $AUC_{0-\infty, norm}$ (*C*) of nintedanib following single oral administration of nintedanib 100, 150, or 200 mg in patients with a body surface area <1.5 m² or ≥1.5 m². $AUC_{0-\infty, norm}$, dose-normalized area under the concentration–time curve (0–∞ hours); $AUC_{0-12, norm}$, dose-normalized area under the concentration–time curve (0–12 hours); $C_{max, norm}$, dose-normalized peak concentration; gMean, geometric mean; BSA, body surface area.

was related to DLTs in three patients and early withdrawal of consent in one patient. Among 38 assessable patients, 10 had a partial response (two patients in the N150/D60 cohort, five in the N150/D75 cohort, two in the N200/D60 cohort, and one in the N200/D75 cohort), yielding an overall response rate of 26.3% (95% confidence interval [CI]: 13.4–43.1%) (Supplemental Table S3, SDC 1, http://links.lww.com/JTO/A737). All 10 responders had nonsquamous histology: nine with adenocarcinoma and one with large-cell carcinoma. A further 18 patients (47.4%) had stable disease, yielding a disease control rate of 73.7%. Median PFS was 5.7 months [95% CI: 4.3–8.3 months].

DISCUSSION

This phase I trial was conducted to determine the MTD of nintedanib in combination with docetaxel in Japanese patients with advanced NSCLC who had previously received platinum-based chemotherapy. The MTD of nintedanib was 150 and 200 mg bid in patients with BSA less than 1.5 and BSA greater than or equal to 1.5 in combination with 75 mg/m² of docetaxel, respectively. The protocol was amended so that patients were divided according to BSA (<1.5 m² and ≥1.5 m²) due to the occurrence of an unexpectedly high number of DLTs in patients with a lower BSA (i.e., <1.5 m²). All DLTs were grade 3 liver enzyme elevations (ALT, AST, or γ-GT), and were completely reversible with dose reduction or discontinuation. A reduced dose of nintedanib was successfully reintroduced following rapid recovery of enzyme levels for eight of 12 patients who had developed liver enzyme level-related DLTs.

All three patients with BSA less than 1.5 treated with nintedanib 200 mg experienced DLTs, whereas only four of 12 patients with BSA greater than or equal to 1.5 treated at the same dose developed DLTs. This is consistent with our previous phase I study of nintedanib monotherapy, in which three of four patients with BSA less than 1.5 in the 200 mg bid cohort developed DLTs (grade 3 hepatic enzyme elevations), whereas DLTs were not reported in eight patients with BSA greater than or equal to 1.5 treated at the same dose.[11]

Studies with other small-molecule tyrosine kinase inhibitors also suggest that dosing according to BSA might be meaningful. For example, a low BSA has been associated with a high incidence of severe toxicities and DLTs in patients treated with sunitinib.[16,17] Furthermore, a reduced dose of 300 mg/day imatinib in low-BSA patients with chronic myeloid leukemia showed equivalent efficacy to the standard dose.[18,19] A large-scale PK analysis of imatinib identified a weak inverse correlation between trough concentration of imatinib and BSA.[20] Based on these observations, larger-scale investigations are warranted to identify optimal initial dosing of nintedanib, especially in low-BSA patients.

In addition to liver enzyme elevations, common drug-related AEs included hematologic toxicities, alopecia, and gastrointestinal AEs. Many of these toxicities are commonly observed during docetaxel administration.[15] These AEs were reversible and could usually be managed effectively with supportive therapies (except for alopecia). The mild-to-moderate gastrointestinal AEs and asymptomatic, reversible liver enzyme increases are consistent with the established safety/tolerability profile of nintedanib in NSCLC and other tumor types.[10,11,21–25] AEs associated with many other VEGF-targeted tyrosine kinase inhibitors, such as grade 3–4 skin toxicities, hypertension, bleeding, perforation, thromboembolism, and proteinuria,[26] were either absent or infrequent in this study.

The PK profile of nintedanib following docetaxel administration was very similar to that seen in our phase I nintedanib monotherapy study.[11] This suggests that docetaxel has no clinically relevant effect on the PK of nintedanib. Analyses of blood samples taken on day 1 of cycle 1 with docetaxel alone, and day 1 of cycle 2 of docetaxel/nintedanib showed that coadministration of nintedanib did not affect the PK of docetaxel. This is consistent with findings from a phase I study of nintedanib/docetaxel in patients with prostate cancer.[25] In the present study, we found no clear differences in PK data from patients with BSA less than 1.5 and BSA greater than or equal to 1.5. This could be due to the small sample size, so population-based PK analyses of nintedanib are needed.

Our study showed that 26% of patients achieved an objective response to nintedanib/docetaxel, with a median PFS of 5.7 months. This high level of antitumor activity is

consistent with data from the global LUME-Lung 1 trial of nintedanib/docetaxel in NSCLC, where a statistically significant improvement in PFS was observed in all patients, and a significant extension in overall survival was seen in patients with adenocarcinoma.[10]

In conclusion, the MTD for continuous daily treatment with nintedanib plus docetaxel (75 mg/m^2) was 150 and 200 mg bid in patients with BSA less than 1.5 and BSA greater than or equal to 1.5, respectively. There were no clinically relevant PK interactions between nintedanib and docetaxel. DLTs were observed in one-third of enrolled patients, and there were two fatal events including hemoptysis; therefore, careful observation of patients receiving nintedanib in combination with docetaxel is required in future investigations.

ACKNOWLEDGMENTS

The authors were fully responsible for all content and editorial decisions, were involved at all stages of manuscript development, and have approved the final version. Medical writing assistance, supported financially by Boehringer Ingelheim, was provided by Duncan Campbell of GeoMed during the preparation of this manuscript.

REFERENCES

1. National Comprehensive Cancer Network®. NCCN Clinical Practice Guidelines in Oncology (NCCN Guidelines®): Non-Small Cell Lung Cancer, version 4. Available at: http://www.nccn.org/. Accessed August 31, 2014.
2. Makrilia N, Lappa T, Xyla V, Nikolaidis I, Syrigos K. The role of angiogenesis in solid tumours: an overview. *Eur J Intern Med* 2009;20:663–671.
3. Sandler A, Gray R, Perry MC, et al. Paclitaxel–carboplatin alone or with bevacizumab for non-small-cell lung cancer. *N Engl J Med* 2006;355:2542–2550.
4. Soria JC, Mauguen A, Reck M, et al.; Meta-Analysis of Bevacizumab in Advanced NSCLC Collaborative Group. Systematic review and meta-analysis of randomised, phase II/III trials adding bevacizumab to platinum-based chemotherapy as first-line treatment in patients with advanced non-small-cell lung cancer. *Ann Oncol* 2013;24:20–30.
5. Amini A, Masoumi Moghaddam S, Morris DL, Pourgholami MH. The critical role of vascular endothelial growth factor in tumor angiogenesis. *Curr Cancer Drug Targets* 2012;12:23–43.
6. Carmeliet P, Jain RK. Angiogenesis in cancer and other diseases. *Nature* 2000;407:249–257.
7. Raica M, Cimpean AM. Platelet-derived growth factor (PDGF)/PDGF receptors (PDGFR) axis as target for antitumor and antiangiogenic therapy. *Pharmaceuticals* 2010;3:572–599.
8. Saylor PJ, Escudier B, Michaelson MD. Importance of fibroblast growth factor receptor in neovascularization and tumor escape from antiangiogenic therapy. *Clin Genitourin Cancer* 2012;10:77–83.
9. Hilberg F, Roth GJ, Krssak M, et al. BIBF 1120: triple angiokinase inhibitor with sustained receptor blockade and good antitumor efficacy. *Cancer Res* 2008;68:4774–4782.
10. Reck M, Kaiser R, Mellemgaard A, et al.; LUME-Lung 1 Study Group. Docetaxel plus nintedanib versus docetaxel plus placebo in patients with previously treated non-small-cell lung cancer (LUME-Lung 1): a phase 3, double-blind, randomised controlled trial. *Lancet Oncol* 2014;15:143–155.
11. Okamoto I, Kaneda H, Satoh T, et al. Phase I safety, pharmacokinetic, and biomarker study of BIBF 1120, an oral triple tyrosine kinase inhibitor in patients with advanced solid tumors. *Mol Cancer Ther* 2010;9:2825–2833.
12. Mross K, Stefanic M, Gmehling D, et al. Phase I study of the angiogenesis inhibitor BIBF 1120 in patients with advanced solid tumors. *Clin Cancer Res* 2010;16:311–319.
13. Gandara DR, Kawaguchi T, Crowley J, et al. Japanese–US common-arm analysis of paclitaxel plus carboplatin in advanced non-small-cell lung cancer: a model for assessing population-related pharmacogenomics. *J Clin Oncol* 2009;27:3540–3546.
14. Maruyama R, Nishiwaki Y, Tamura T, et al. Phase III study, V-15-32, of gefitinib versus docetaxel in previously treated Japanese patients with non-small-cell lung cancer. *J Clin Oncol* 2008;26:4244–4252.
15. TAXOTERE [package inserts]. Bridgewater, NJ: sanofi-aventis U.S. LLC; 2013.
16. Huillard O, Mir O, Peyromaure M, et al. Sarcopenia and body mass index predict sunitinib-induced early dose-limiting toxicities in renal cancer patients. *Br J Cancer* 2013;108:1034–1041.
17. van der Veldt AA, Boven E, Helgason HH, et al. Predictive factors for severe toxicity of sunitinib in unselected patients with advanced renal cell cancer. *Br J Cancer* 2008;99:259–265.
18. Park SJ, Choi IK, Seo HY, et al. Reduced dose of imatinib for patients with chronic myeloid leukemia and low body surface area. *Acta Haematol* 2007;118:219–221.
19. Sakai M, Miyazaki Y, Matsuo E, et al. Long-term efficacy of imatinib in a practical setting is correlated with imatinib trough concentration that is influenced by body size: a report by the Nagasaki CML Study Group. *Int J Hematol* 2009;89:319–325.
20. Larson RA, Druker BJ, Guilhot F, et al.; IRIS (International Randomized Interferon vs STI571) Study Group. Imatinib pharmacokinetics and its correlation with response and safety in chronic-phase chronic myeloid leukemia: a subanalysis of the IRIS study. *Blood* 2008;111:4022–4028.
21. Doebele RC, Conkling P, Traynor AM, et al. A phase I, open-label dose-escalation study of continuous treatment with BIBF 1120 in combination with paclitaxel and carboplatin as first-line treatment in patients with advanced non-small-cell lung cancer. *Ann Oncol* 2012;23:2094–2102.
22. Ellis PM, Kaiser R, Zhao Y, Stopfer P, Gyorffy S, Hanna N. Phase I open-label study of continuous treatment with BIBF 1120, a triple angiokinase inhibitor, and pemetrexed in pretreated non-small cell lung cancer patients. *Clin Cancer Res* 2010;16:2881–2889.
23. Ledermann JA, Hackshaw A, Kaye S, et al. Randomized phase II placebo-controlled trial of maintenance therapy using the oral triple angiokinase inhibitor BIBF 1120 after chemotherapy for relapsed ovarian cancer. *J Clin Oncol* 2011;29:3798–3804.
24. Reck M, Kaiser R, Eschbach C, et al. A phase II double-blind study to investigate efficacy and safety of two doses of the triple angiokinase inhibitor BIBF 1120 in patients with relapsed advanced non-small-cell lung cancer. *Ann Oncol* 2011;22:1374–1381.
25. Bousquet G, Alexandre J, Le Tourneau C, et al. Phase I study of BIBF 1120 with docetaxel and prednisone in metastatic chemo-naive hormone-refractory prostate cancer patients. *Br J Cancer* 2011;105:1640–1645.
26. Boehm S, Rothermundt C, Hess D, Joerger M. Antiangiogenic drugs in oncology: a focus on drug safety and the elderly—a mini-review. *Gerontology* 2010;56:303–309.

Multiple regulatory mechanisms of hepatocyte growth factor expression in malignant cells with a short poly(dA) sequence in the HGF gene promoter

KAZUKO SAKAI[1], MASAYUKI TAKEDA[2], ISAMU OKAMOTO[3], KAZUHIKO NAKAGAWA[2] and KAZUTO NISHIO[1]

Departments of [1]Genome Biology and [2]Medical Oncology, Faculty of Medicine, Kinki University, Osaka-Sayama, Osaka 589-8511; [3]Center for Clinical and Translational Research, Kyushu University Hospital, Fukoka, Kyushu 812-8581, Japan

Received February 15, 2014; Accepted October 15, 2014

DOI: 10.3892/ol.2014.2702

Abstract. Hepatocyte growth factor (HGF) expression is a poor prognostic factor in various types of cancer. Expression levels of HGF have been reported to be regulated by shorter poly(dA) sequences in the promoter region. In the present study, the poly(dA) mononucleotide tract in various types of human cancer cell lines was examined and compared with the HGF expression levels in those cells. Short deoxyadenosine repeat sequences were detected in five of the 55 cell lines used in the present study. The H69, IM95, CCK-81, Sui73 and H28 cells exhibited a truncated poly(dA) sequence in which the number of poly(dA) repeats was reduced by ≥5 bp. Two of the cell lines exhibited high HGF expression, determined by reverse transcription quantitative polymerase chain reaction and enzyme-linked immunosorbent assay. The CCK-81, Sui73 and H28 cells with shorter poly(dA) sequences exhibited low HGF expression. The cause of the suppression of HGF expression in the CCK-81, Sui73 and H28 cells was clarified by two approaches, suppression by methylation and single nucleotide polymorphisms in the *HGF* gene. Exposure to 5-Aza-dC, an inhibitor of DNA methyltransferase 1, induced an increased expression of HGF in the CCK-81 cells, but not in the other cells. Single-nucleotide polymorphism (SNP) rs72525097 in intron 1 was detected in the Sui73 and H28 cells. Taken together, it was found that the defect of poly(dA) in the *HGF* promoter was present in various types of cancer, including lung, stomach, colorectal, pancreas and mesothelioma. The present study proposes the negative regulation mechanisms by methylation and SNP in intron 1 of *HGF* for HGF expression in cancer cells with short poly(dA).

Correspondence to: Dr Kazuto Nishio, Department of Genome Biology, Faculty of Medicine, Kinki University, 377-2 Ohnohigashi, Osaka-Sayama, Osaka 589-8511, Japan
E-mail: knishio@med.kindai.ac.jp

Key words: hepatocyte growth factor, poly(dA), deletion, methylation, cancer

Introduction

Hepatocyte growth factor (HGF) is a widely-expressed multifunctional growth and angiogenic factor (1). The activity of HGF is mediated by binding to its receptor, a tyrosine kinase MET, and HGF transduces multiple biological effects in target cells, including adhesion, motility, growth, survival and morphogenesis (2).

The HGF level is frequently increased in advanced cancer patients. HGF is a poor prognostic factor of patients with various types of cancer, including hepatocellular carcinoma and breast cancer (3-5). In addition, HGF is reported to be associated with resistance to molecular target drugs, including EGFR-specific tyrosine kinase inhibitors, in lung cancer (6,7). HGF is secreted by tumor cells, vascular smooth muscle cells, pericytes and fibroblasts. The *HGF* gene promoter in humans and mice has been structurally and functionally analyzed (8-10). Inflammatory cytokines, including interleukin-1- and interleukin-6-responsive elements, are present in the human *HGF* gene (8), which is activated transcriptionally by these cytokines. However, little is known about genomic alteration associated with the expression of HGF. Ma *et al* reported that high expression of HGF is regulated by a short deletion in the poly(dA) repeat sequence in the *HGF* promoter region in breast cancer cells (11). The present study investigated the association between the expression levels of HGF in those cells and additional regulation mechanisms of HGF expression.

Materials and methods

Cells and cell culture. Human non-small cell lung cancer (NSCLC) PC-6, PC-7, PC-9 and PC-14 cell lines were provided by Tokyo Medical University (Tokyo, Japan) (12,13). The NSCLC SBC-3 cell line was provided by Okayama University School of Medicine (Okayama, Japan) (13). The NSCLC N231, LK-2, Ma-1 and 11_18 cell lines were provided by the National Cancer

Research Institute (Tokyo, Japan) (14-17). The NSCLC A549, H1299, H69, Calu-1, Calu-6, H292, H358, H441, H460, H2087, H1650, H1838, H1975 and HCC827 cell lines were obtained from the American Type Culture Collection (Mannassas, VA, USA). The NSCLC EBC-1 cell line was obtained from the Japanese Collection of Research Bioresources Cell Bank (Osaka, Japan). Human gastric cancer HSC38, HSC43 and HSC58 cell lines were provided by the National Cancer Center Research Institute (18,19). Human gastric cancer cell line, OKAJIMA, was provided by Osaka City University (Osaka, Japan). Human gastric cancer IM95, MKN1, MKN7 and MKN74 cell lines were obtained from the Japanese Collection of Research Bioresources Cell Bank. Human gastric cancer N87 and SNU16 cell lines and pancreatic cancer MIAPaCa cell lines were obtained from the American Type Culture Collection. Human pancreatic cancer Sui87, Sui68, Sui70 and Sui73 cell lines were provided by the National Cancer Center Research Institute (20). Human colon cancer HCC56, SW837, CCK-81, Colo201, Colo320 and WiDr cell lines and human hepatocellular cancer HLE, HLF and Huh7 cell lines were obtained from the Japanese Collection of Research Bioresources Cell Bank. Human hepatocellular cancer HepG2, human breast cancer MDAMB-468 and BT-549 cell lines, the human glioma U251 cell line, the human prostate PC-3 cancer cell line and human mesothelioma H28 and MSTO cell lines were obtained from the American Type Culture Collection. The cell lines were maintained in RPMI-1640 medium supplemented with 10% heat-inactivated fetal bovine serum (FBS; Equitech-Bio, Inc., Kerrville, TX, USA). All cell lines were maintained in a 5% CO_2, humidified atmosphere at 37˚C.

Sample preparation. Total RNA was extracted from cells using ISOGEN (Nippon Gene Co., Ltd., Tokyo, Japan), according to the manufacturer's instructions. The cDNA templates were synthesized from 1 μg of total RNA using the GeneAmp® RNA polymerase chain reaction (PCR) kit (Applied Biosystems, Foster City, CA, USA).

DNA was extracted from cells using the QIAamp DNA mini kit (Qiagen, Valencia, CA, USA), according to the manufacturer's instructions. For the 10 mM stock solution, 5-Aza-2'-deoxycytidine (5-Aza-dC; Sigma-Aldrich, St. Louis, MO, USA) was dissolved in dimethylsulfoxide. Aliquots were prepared and frozen at -80˚C. The cells were treated with 5-Aza-dC for 48 h prior to the cells being collected and total RNA extracted.

Reverse transcription-quantitative PCR (RT-qPCR). The methods used in the present section have been previously described (21). Briefly, RT-qPCR was performed by using a Premix Ex Taq and Smart Cycler system (Takara Bio, Inc., Shiga, Japan), according to the manufacturer's instructions. The primers used for RT-qPCR were purchased from Takara Bio, Inc. and were as follows: Forward, 5'-GTAAATGGGATTCCAACACGAACAA-3' and reverse, 5'-TGTCGTGCAGTAAGAACCCAACTC-3' for *HGF*; forward, 5'-GCACCGTCAAGGCTGAGAAC-3' and reverse, 5'-ATGGTGGTGAAGACGCCAGT-3' for glyceraldehyde-3-phosphate dehydrogenase (*GAPDH*). The cDNA was then used as the template for the qPCR reaction. The PCR conditions were as follows: one cycle at 95˚C for 5 min, followed by 40 cycles at 95˚C for 10 sec and 60˚C for 30 sec. The threshold cycle (Ct) values were determined using Thermal Cycler Dice Real Time System (Takara Bio, Inc.). The experiment was independently performed in triplicate using *GAPDH* as a reference to normalize the data.

Enzyme-linked immunosorbent assay (ELISA). The cells were seeded at a density of $2x10^6$ cells per 10-cm dish in medium supplemented with 10% FBS and were cultured for 24 h. The medium was then changed to serum-free medium. Following 48 h of incubation, the conditioned medium was collected to measure HGF production.

HGF concentrations in the cultured medium were determined using a Human HGF Quantikine ELISA kit (R&D Systems, Inc., Minneapolis, MN, USA) according to the manufacturer's instructions. The absorbance of the samples at 450 nm was measured using VERSAmax (Molecular Devices Japan K.K, Tokyo, Japan). Duplicate examinations of 50 μl of the cell-conditioned medium were performed.

DNA amplification and fragment sizing. DNA amplification was performed with Ex Taq polymerase (Takara Bio, Inc.). The cycling program was one cycle of 98˚C for 1 min and then 30 cycles of 98˚C for 10 sec, 60˚C for 30 sec and 72˚C for 10 sec, followed by one cycle of 72˚C for 2 min. PCR fragments of 88 bp were analyzed using the Agilent 2100 bioanalyzer (Agilent Technologies, Palo Alto, CA, USA). The primers used for PCR amplification were as follows, forward, 5'-GGTAAATGTGTGGTATTTCGT GAG-3' and reverse, 5'-GCTGCCTGCTCTGAGCCCAT-3'.

Sequencing analysis. DNA sequencing was performed directly on purified PCR products using the BigDye terminator v 3.1 sequencing kit (Applied Biosystems). DNA amplification was performed with Ex Taq polymerase (Takara Bio, Inc.). The cycling program was one cycle at 98˚C for 1 min and then 30 cycles at 98˚C for 10 sec, 60˚C for 30 sec and 72˚C for 1 min, followed by one cycle at 72˚C for 2 min. Following PCR, the product was purified using the QIAquick PCR purification kit (Qiagen), and then sequenced using the ABI BigDye 3.1 dye terminator V3.1 kit (Applied Biosystems) on an ABI Prism® 3100 DNA Analyzer automated sequencer (Applied Biosystems). The primer and probe sequences used were as follows: Forward primer, 5'-TGTGATTCTTCTCCTCGTGGGGT-3', reverse primer, 5'-AGCCTGACCGTGACCCTGAA-3' and sequencing primer, 5'-AGCCTGACCGTGACCCTGAA-3', for rs11763015 and rs78601897; forward primer, 5'-TGTGATTCTTCTCCTCG TGGGGT-3', reverse primer, 5'-CCAAGAAACAGTCATTGTC CATAGCCTGTCCC-3' and sequencing primer, 5'-CCTGGGG ACACCAGACAGAGGCTG-3', for rs3735520 and rs3735521; forward primer, 5'-GCATATTCAGTACTCACGAATTCAA-3', reverse primer, 5'-TGGGACGGGGCTTGGGTTGGA-3' and sequencing primer, 5'-CCAGGCATCTCCTCCAGAGGGAT CCG-3', for rs72525097.

Results

Sequencing of the poly(dA) repeat in the HGF promoter region. The HGF promoter region contains a poly(dA) repeat at

Table I. A list of single nucleotide polymorphisms detected in the 12 cell lines. The poly(dA) length represents the number of deoxyadenosine repeat sequences in the *HGF* gene from the results of direct sequencing. HGF production represents the results of the enzyme-linked immunosorbent assay.

Cell line	poly(dA) length	HGF production (pg/ml)	rs11763015-2142C/A	rs78601897-1903G/A	rs3735520-1652C/T	rs3735521-1268G/C	rs72525097 247(-/T)
H69	24	2443.0	C	G	C	G	-
IM95	17	11297.6	C/A	G	T	G	-
Sui73	17	3.6	C	G	C/T	G	T
CCK-81	16	10.0	C	G	C	G	-
H28	20	6.2	C	G	C/T	G	T
A549	27	26.2	C	G	C	G	-
PC-9	29	3.1	C	G	C	G	-
H1975	28	14.4	C	G	C	G	-
HCC827	28	NT	C	G	C/T	G	-
H1650	29	NT	C	G	C	G	-
11_18	29	NT	C	G	C/T	G	-
Ma-1	28	NT	C	G	C	G	-

NT, not tested; HGF, hepatocyte growth factor.

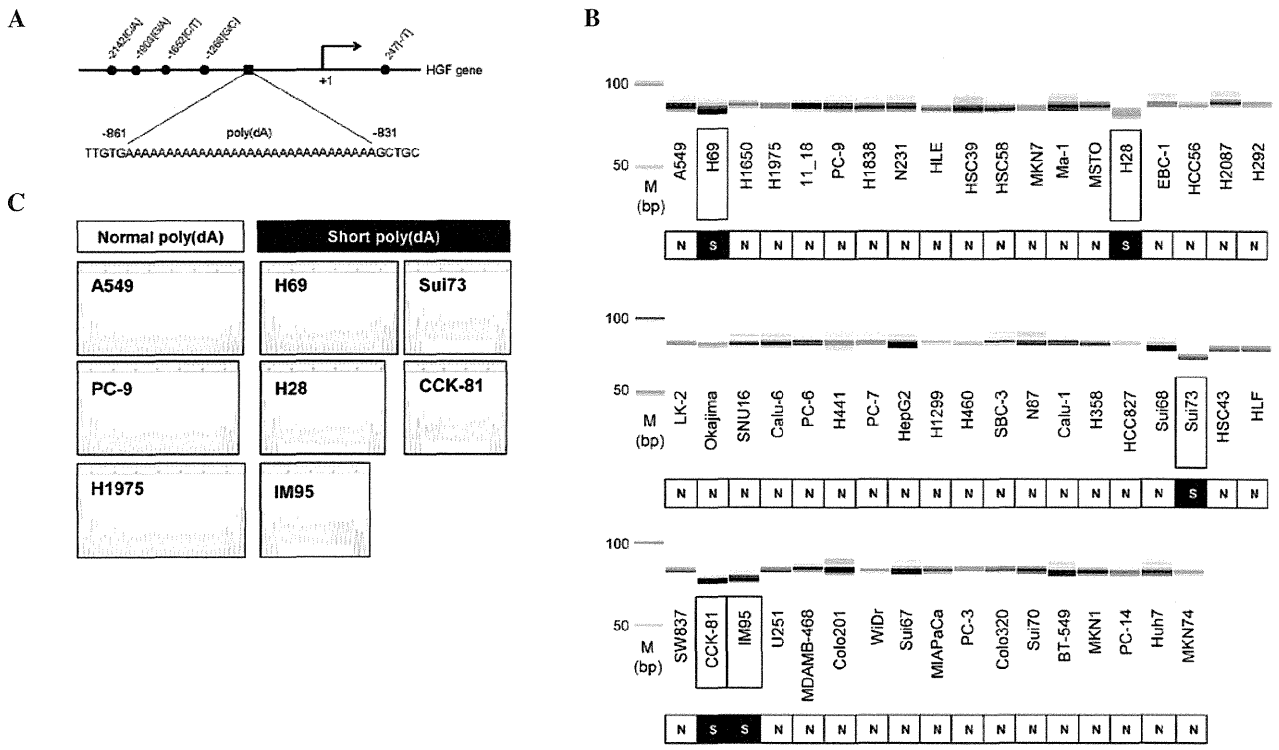

Figure 1. (A) Schematic representation of the human hepatocyte growth factor promoter. The square (■) and circle (●) show the location of poly(dA) and single-nucleotide polymorphisms, respectively. (B) Capillary electrophoresis of reverse transcription-polymerase chain reaction products derived from 55 cell lines. The product from the A549 cell line [normal poly(dA)] was applied for each assay as a control. DNA size standards (100 and 50 bp) are shown on the left. Truncated fragments were detected in the H69, IM95, CCK-81, Sui73 and H28 cell lines. (C) DNA sequencing of the poly(dA) region in the eight cell lines. Sequencing analysis revealed the truncated fragment of the poly(dA) sequence in the H69, IM95, CCK-81, Sui73 and H28 cell lines. The dominant peak represents the true fragment length. The right end peaks likely represent polymerase slippage.

~800 bp upstream from the translation initiation site (Fig. 1A). Based on a previous study (11), the poly(dA) lengths were analyzed by fragment sizing in 55 human cancer cell lines. Shorter fragments were detected in the Sui73, CCK81, IM95, H69 and H28 cells, but not in the remaining cell lines (Fig. 1B). To confirm the fragment size, the poly(dA) region of eight cell

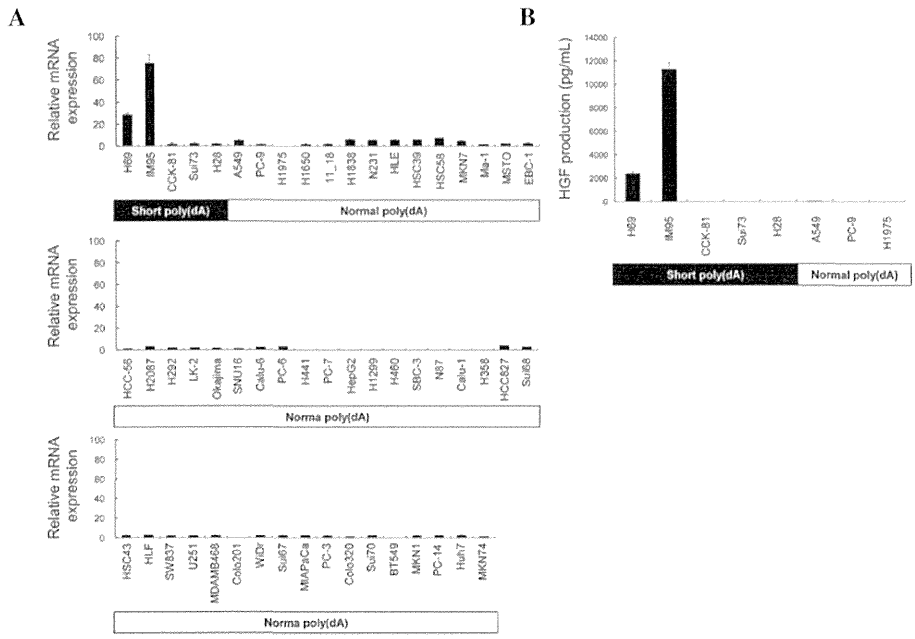

Figure 2. (A) Expression of *HGF* mRNA in human cancer cell lines. cDNA (4 ng RNA/μl; 1 μl) was used for the quantitative polymerase chain reaction. Relative *HGF* mRNA in the each cell lines were normalized by glyceraldehyde-3-phosphate dehydrogenase mRNA levels. The experiment was performed in triplicate, and repeated three times independently. The data are expressed as the mean ± standard deviation of triplicate samples. (B) Production of HGF protein by the eight cell lines. Each cell line was cultured in the medium. HGF concentration in the conditioned medium was determined by enzyme-linked immunosorbent assay. The experiment was performed in triplicate. HGF, hepatocyte growth factor

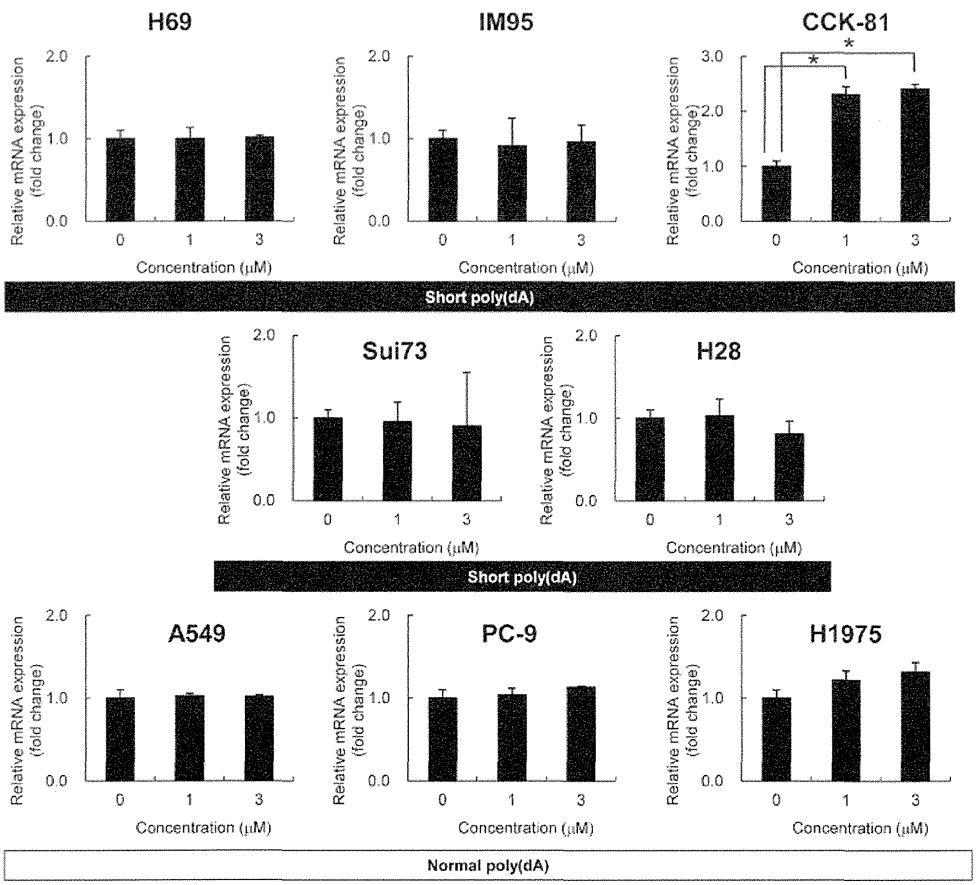

Figure 3. Induction of *HGF* mRNA expression by 5Aza-dC treatment in eight cell lines. The indicated cell lines were treated with 1 or 3 μM 5Aza-dC for 48 h, and total RNA was prepared. Levels of *HGF* and *GAPDH* mRNA were quantified by reverse transcription-quantitative polymerase chain reaction. Relative HGF mRNA was normalized by glyceraldehyde-3-phosphate dehydrogenase mRNA levels. The experiment was performed in triplicate, and repeated three times independently. The data are expressed as the mean ± standard deviation of triplicate samples. *P<0.01 by Student's t-test. HGF, hepatocyte growth factor.

lines was sequenced (Fig. 1C). The number of mononucleotide repeats in these cell lines matched with the result of the fragment analysis.

HGF expression in human cancer cells. The levels of *HGF* expression in 55 cell lines were then examined by RT-qPCR (Fig. 2A). RT-qPCR analysis revealed a low expression in the majority of the cell lines. On the other hand, the H69 and IM95 cells expressed high levels of *HGF* mRNA. The expression of HGF mRNA in the H69 and IM95 cells was >12.3- and >32.4-fold higher compared with the average of any cell line other than H69 or IM95, respectively. HGF protein secretion was examined in the eight cell lines (Fig. 2B). The HGF protein was highly secreted by H69 and IM95 cells in the conditioned medium, which was consistent with mRNA expression.

The pattern of poly(dA) length (Fig 1B) and *HGF* expression (Fig. 2A) was compared in 55 cell lines. The expression level of *HGF* was low in all the cell lines with a normal poly(dA) length in the *HGF* promoter region. By contrast, *HGF* expression in the five cell lines with short poly(dA) length in the *HGF* promoter region differed in pattern. High expression of *HGF* was observed in the H69 and IM95, but not in the CCK-81, Sui73, and H28 cell lines. These results suggest that the cell lines with a normal poly(dA) promoter express low levels of *HGF*, and all cell lines with a short poly(dA) do not express high levels of *HGF*. It was hypothesized that the *HGF* expression was suppressed in the CCK-81, Sui73 and H28 cells with short poly(dA) by other mechanisms.

Effect of 5-Az-dC on HGF expression. The present study explored the cause of *HGF* gene suppression in certain cell lines with shorter poly(dA) sequences. It was hypothesized that DNA methylation may silence *HGF* expression in these cell lines. The change in the *HGF* mRNA expression in three cell lines was examined following treatment with 1 or 3 μM 5-Aza-dC for 48 h (Fig. 3). A 2.3- and 2.4-fold increase in *HGF* mRNA was observed in CCK-81 cells when treated with 1 and 3 μM 5-Aza-dC, respectively ($P<0.01$). No significant change was observed in the Sui73 and H28 cells. These results suggest that DNA methylation may contribute to the silencing of the *HGF* gene in the CCK-81 cells.

Genotyping of SNPs in the HGF gene. All increased expression of *HGF* in the Sui73 and H28 cells was due to DNA methylation. Next, it was examined whether a specific polymorphism is observed in these cells. The *HGF* genotypes were analyzed upstream of the transcript start (-2200 bp) to intron1 (+300 bp) of 12 cell lines with short poly(dA) (H69, IM95, CCK-81, Sui73, and H28 cells) or normal poly(dA) (A549, PC-9, H1975, HCC827, H1650, 11_18, and Ma-1 cells) by direct sequencing (Table I). The -1903G and -1268G SNPs were detected in all 12 cell lines. The -2142C/A SNP was detected in only the IM95 cell line with short poly(dA). The -1652C/T SNP was detected in four cell lines with shorter and normal poly(dA). The +247T SNP in intron 1 was detected in only the Sui73 and H28 cells with a short poly(dA). These results suggest that insertion of a single T nucleotide at position 247 may be associated with the expression of HGF in the Sui73 and H28 cells with a short poly(dA).

Discussion

HGF has been identified as a natural ligand of the MET receptor and belongs to the plasminogen family (1). In cancer cells, activation of the MET receptor increases invasion and metastasis, and allows the survival of cancer cells in the bloodstream in the absence of anchorage (2).

In the present study, the deletion mutation on the HGF promoter region was detected in lung, colon, stomach, pancreatic and mesothelial cancer cell lines. The cell lines with short poly(dA) express high levels of *HGF*, whereas all the cell lines with normal poly(dA) do not. This result is consistent with a previous study (11) and short poly(dA) in the *HGF* promoter region has been detected in various types of cancer cell lines and breast cancer. H69 [poly(dA), 24 bp] and IM95 [poly(dA), 17 bp] highly express *HGF*. When comparing these two cell lines, IM95 exhibits a higher *HGF* expression compared with H69 (2.6- and 4.6-fold higher at the mRNA and protein levels, respectively). This is also consistent with the study by Ma *et al*, suggesting that the cells with shorter poly(dA) exhibit higher *HGF* (11).

By contrast, certain cell lines exhibited a short poly(dA) and low *HGF* expression. We considered that the low *HGF* expression in these cell lines may be explained by the methylation or polymorphisms of the *HGF* promoter. There has been no previous paper reporting epigenetic regulation of HGF expression. Recently, DNA methylation analysis of *HGF* promoters was reported. Analysis of bisulfite DNA from BNL 1ME A.7R.1 cells indicated that *HGF* has 35% of CpGs methylated at two sites (22). This finding is considered to be important for elucidating the detailed mechanisms of epigenetic regulation of HGF expression, in order to develop epigenetic therapy for HGF-related cancers.

An increase (by 2.4-fold) in *HGF* expression was induced by 5Aza-dC in Sui73 and H28 cell lines, suggesting that other mechanisms such as acetylation and transcription factors may influence the full expression of HGF.

T insertion in intron 1 (247T) was detected in two cell lines with short poly(dA). It is well-known that polymorphisms in the promoter, but not in introns, influence the transcription of a gene. However, Onouchi *et al* reported that an SNP in intron 1 of 1,4,5-trisphosphate 3-kinase C influenced the transcription of this gene (23). Yamada *et al* reported that polymorphism in intron 1 of transcription factor *EGR3* regulates transcription of this gene (24). Subsequently, it was hypothesized that 247(-/T) may influence the transcriptional levels of HGF in these cell lines, although functional analysis is necessary in future studies. Another SNP was detected in 4/12 cell lines (-1652C/T); however, the influence of this SNP on HGF expression remains unknown.

HGF is an important mediator of epithelial-mesenchymal transition (EMT) (25). Fibroblastic changes in the cells were often observed during EMT induced by HGF and other ligands. The association between SNPs in HGF and EMT may be investigated in future studies.

In conclusion, the present study found that the deletion polymorphism of poly(dA) in the *HGF* promoter was present in various cancer cell lines, including lung, stomach, colorectal and pancreatic cancer, and mesothelioma cell lines. Future experiments with functional analysis of

intron 1 polymorphisms may provide a novel negative regulatory mechanism of *HGF* expression.

Acknowledgements

The present study was supported by the Third-Term Comprehensive 10-Year Strategy for Cancer Control and funds for Health and Labor Scientific Research Grants (20-9), and a Grant-in-Aid for Scientific Research (B) (23701106).

References

1. Naldini L, Vigna E, Narsimhan RP, Gaudino G, Zarnegar R, Michalopoulos GK and Comoglio PM: Hepatocyte growth factor (HGF) stimulates the tyrosine kinase activity of the receptor encoded by the proto-oncogene c-MET. Oncogene 6: 501-504, 1991.
2. Benvenuti S and Comoglio PM: The MET receptor tyrosine kinase in invasion and metastasis. J Cell Physiol 213: 316-325, 2007.
3. Schoenleber SJ, Kurtz DM, Talwalkar JA, Roberts LR and Gores GJ: Prognostic role of vascular endothelial growth factor in hepatocellular carcinoma: systematic review and meta-analysis. Br J Cancer 100: 1385-1392, 2009.
4. Seidel C, Børset M, Turesson I, Abildgaard N, Sundan A and Waage A: Elevated serum concentrations of hepatocyte growth factor in patients with multiple myeloma. The Nordic Myeloma Study Group. Blood 91: 806-812, 1998.
5. Toi M, Taniguchi T, Ueno T, Asano M, Funata N, Sekiguchi K, Iwanari H and Tominaga T: Significance of circulating hepatocyte growth factor level as a prognostic indicator in primary breast cancer. Clin Cancer Res 4: 659-664, 1998.
6. Yano S, Wang W, Li Q, Matsumoto K, Sakurama H, Nakamura T, Ogino H, *et al*: Hepatocyte growth factor induces gefitinib resistance of lung adenocarcinoma with epidermal growth factor receptor-activating mutations. Cancer Res 68: 9479-9487, 2008.
7. Kasahara K, Arao T, Sakai K, Matsumoto K, Sakai A, Kimura H, Sone T, *et al:* Impact of serum hepatocyte growth factor on treatment response to epidermal growth factor receptor tyrosine kinase inhibitors in patients with non-small cell lung adenocarcinoma. Clin Cancer Res 16: 4616-4624.
8. Miyazawa K, Kitamura A and Kitamura N: Structural organization and the transcription initiation site of the human hepatocyte growth factor gene. Biochemistry 30: 9170-9176, 1991.
9. Okajima A, Miyazawa K and Kitamura N: Characterization of the promoter region of the rat hepatocyte-growth-factor/scatter-factor gene. Eur J Biochem 213: 113-119, 1993.
10. Plaschke-Schlütter A, Behrens J, Gherardi E and Birchmeier W: Characterization of the scatter factor/hepatocyte growth factor gene promoter. Positive and negative regulatory elements direct gene expression to mesenchymal cells. J Biol Chem 270: 830-836, 1995.
11. Ma J, DeFrances MC, Zou C, Johnson C, Ferrell R and Zarnegar R: Somatic mutation and functional polymorphism of a novel regulatory element in the HGF gene promoter causes its aberrant expression in human breast cancer. J Clin Invest 119: 478-491, 2009.
12. Nishio K, Arioka H, Ishida T, Fukumoto H, Kurokawa H, Sata M, Ohata M and Saijo N: Enhanced interaction between tubulin and microtubule-associated protein 2 via inhibition of MAP kinase and CDC2 kinase by paclitaxel. Int J Cancer 63: 688-693, 1995.
13. Kawamura-Akiyama Y, Kusaba H, Kanzawa F, Tamura T, Saijo N and Nishio K: Non-cross resistance of ZD0473 in acquired cisplatin-resistant lung cancer cell lines. Lung Cancer 38: 43-50, 2002.
14. Iwasa T, Okamoto I, Suzuki M, Nakahara T, Yamanaka K, Hatashita E, Yamada Y, *et al:* Radiosensitizing effect of YM155, a novel small-molecule survivin suppressant, in non-small cell lung cancer cell lines. Clin Cancer Res 14: 6496-6504, 2008.
15. Okabe T, Okamoto I, Tamura K, Terashima M, Yoshida T, Satoh T, Takada M, *et al:* Differential constitutive activation of the epidermal growth factor receptor in non-small cell lung cancer cells bearing EGFR gene mutation and amplification. Cancer Res 67: 2046-2053, 2007.
16. Takezawa K, Okamoto I, Yonesaka K, Hatashita E, Yamada Y, Fukuoka M and Nakagawa K: Sorafenib inhibits non-small cell lung cancer cell growth by targeting B-RAF in KRAS wild-type cells and C-RAF in KRAS mutant cells. Cancer Res 69: 6515-6521, 2009.
17. Sato M, Takahashi K, Nagayama K, Arai Y, Ito N, Okada M, Minna JD, *et al:* Identification of chromosome arm 9p as the most frequent target of homozygous deletions in lung cancer. Genes Chromosomes Cancer 44: 405-414, 2005.
18. Yanagihara K, Seyama T, Tsumuraya M, Kamada N and Yokoro K: Establishment and characterization of human signet ring cell gastric carcinoma cell lines with amplification of the c-myc oncogene. Cancer Res 51: 381-386, 1991.
19. Yanagihara K, Tanaka H, Takigahira M, Ino Y, Yamaguchi Y, Toge T, Sugano K and Hirohashi S: Establishment of two cell lines from human gastric scirrhous carcinoma that possess the potential to metastasize spontaneously in nude mice. Cancer Sci 95: 575-582, 2004.
20. Yanagihara K, Takigahira M, Tanaka H, Arao T, Aoyagi Y, Oda T, Ochiai A and Nishio K: Establishment and molecular profiling of a novel human pancreatic cancer panel for 5-FU. Cancer Sci 99: 1859-1864, 2008.
21. Kaneda H, Arao T, Tanaka K, Tamura D, Aomatsu K, Kudo K, Sakai K, *et al:* FOXQ1 is overexpressed in colorectal cancer and enhances tumorigenicity and tumor growth. Cancer Res 70: 2053-2063, 2010.
22. Ogunwobi OO, Puszyk W, Dong HJ and Liu C: Epigenetic upregulation of HGF and c-Met drives metastasis in hepatocellular carcinoma. PLoS One 8: e63765, 2013.
23. Onouchi Y, Gunji T, Burns JC, Shimizu C, Newburger JW, Yashiro M, Nakamura Y, *et al:* ITPKC functional polymorphism associated with Kawasaki disease susceptibility and formation of coronary artery aneurysms. Nat Genet 40: 35-42, 2008.
24. Yamada K, Gerber DJ, Iwayama Y, Ohnishi T, Ohba H, Toyota T, Aruga J, *et al:* Genetic analysis of the calcineurin pathway identifies members of the EGR gene family, specifically EGR3, as potential susceptibility candidates in schizophrenia. Proc Natl Acad Sci USA 104: 2815-2820, 2007.
25. Grotegut S, von Schweinitz D, Christofori G and Lehembre F: Hepatocyte growth factor induces cell scattering through MAPK/Egr-1-mediated upregulation of Snail. EMBO J 25: 3534-3545, 2006.